

Development of a magnetic micro-robotic system and micro
agent's motion control through visual feedback



Author

MUHAMMAD ZOHAIB AKRAM

Reg. Number

00000317813

Supervisor

DR. DANISH HUSSAIN

DEPARTMENT OF MECHATRONICS ENGINEERING
COLLEGE OF ELECTRICAL & MECHANICAL ENGINEERING
NATIONAL UNIVERSITY OF SCIENCES AND TECHNOLOGY
ISLAMABAD
SEPTEMBER 2021

Development of a magnetic micro-robotic system and micro
agent's motion control through visual feedback

Author

MUHAMMAD ZOHAIB AKRAM

Regn Number

00000317813

A thesis submitted in partial fulfillment of the requirements for the degree of
MS Mechatronics Engineering

Thesis Supervisor:

DR. DANISH HUSSAIN

Thesis Supervisor's Signature: _____

DEPARTMENT OF MECHATRONICS ENGINEERING
COLLEGE OF ELECTRICAL & MECHANICAL ENGINEERING
NATIONAL UNIVERSITY OF SCIENCES AND TECHNOLOGY,
ISLAMABAD
September 2021

Declaration

I certify that this research work titled “*Development of a magnetic micro-robotic system and micro agent’s motion control through visual feedback*” is my work. The work has not been presented elsewhere for assessment. The material that has been used from other sources has been properly acknowledged/referred to.

Signature of Student
Muhammad Zohaib Akram
NS 00000317813

Language Correctness Certificate

This thesis has been read by an English expert and is free of typing, syntax, semantic, grammatical, and spelling mistakes. The thesis is also according to the format given by the university.

Signature of Student

MUHAMMAD ZOHAIB AKRAM

Registration Number

00000317813

Signature of Supervisor

Copyright Statement

- Copyright in the argument of this apriorism rests with the apprentice author. Copies (by any process) either in abounding or of extracts, may be fabricated only afterward instructions accustomed by the columnist and lodged in the Library of NUST College of E&ME. Details may be acquired by the Librarian. This folio must anatomy part of any such copies made. Further copies (by any process) may not be fabricated without the permission (in writing) of the author
- The buying of any bookish property rights which may be declared in this apriorism is vested in NUST College of E&ME, accountable to any above-mentioned agreement to the contrary, and may not be fabricated available for use by third parties after the accounting permission of the College of E&ME, which will appoint the acceding and altitude of any such agreement
- Further advice on the altitude under which disclosures and corruption may booty place is accessible from the Library of NUST College of E&ME, Rawalpindi.

Acknowledgments

I am beholden to my Creator Allah Subhana-Watala for guidance, through accomplished my activity and apriorism at every date and for every new anticipation which you set up in my apperception to advance it. Indeed, I could accept done annihilation without your priceless advice and guidance. Whosoever helped me throughout my thesis, whether my parents or any added individual was your will, so absolutely none be aces of acclaim but you. I am abundantly thankful to my admired parents and my affinity who aloft me back I was not able of walking and connected to abutment me throughout every administration of my life. I would additionally like to accurate special acknowledgment to supervisor Dr. Danish Hussain for his advice throughout my apriorism and additionally the Micro/Nano Robotics courses that he has accomplished me. I can cautiously say that I haven't abstruse any added engineering accountable in such abyss as the ones which he has taught. I would additionally like to pay appropriate thanks to my Co-supervisor Dr. Anas Bin Aqeel for his tremendous abutment and cooperation. Each time I got ashore in something; he came up with the solution. After his help, I wouldn't accept been able to complete my thesis.

I acknowledge his backbone and advice throughout the accomplished thesis. I would additionally like to acknowledge Dr. Hamid Jabbar and Dr. Mubashir Saleem for their actuality on my thesis advice and appraisal committee and accurate my appropriate Thanks to Miss Aiman Fatima for his help. I am also beholden to Mr. Ayaz Fayyaz, Zain, and Usman Khan for their abutment and cooperation.

Finally, I would like to accurate my acknowledgment to all the individuals who accept rendered admired assistance to my study.

Dedicate to my aberrant parents and siblings whose amazing support and cooperation led me to this admirable accomplishment

Abstract

Micro robotics is a fast-growing field with a wide spectrum of applications which include biomedical, surveillance, defense, space exploration, geological exploration, environmental monitoring, and oil seepage cleaning to name a few. These robots are actuated through wireless power sources such as light, electrostatic, electrophoretic, dielectrophoretic, and magnetic or they can be chemically self-propelled. Magnetic actuation is widely used because of its long-range, cost-effectiveness, and biocompatibility at low frequencies. Magnetic actuators are constructed using Maxwell, Helmholtz, and cylindrical coils. A Helmholtz coil and Maxwell coil pair can generate a uniform magnetic field and uniform magnetic gradient along its central axis respectively. uniform magnetic gradient fields or uniform magnetic fields are used to actuate and control the movement of microrobots. By using one or more of these types of coils, 1D, 2D, 3D, or multiple degrees of freedom micro-robotic systems are developed. Numerous kinds of feedbacks such as visual feedback, ultrasonic feedback, and hepatic feedback are used for precise motion control.

This dissertation investigates the various parameters that influence the magnetic field produced by a magnetic actuator, based upon the established theories, and proposes a technique to fabricate and optimize the actuation system and electromagnetic actuators. To produce an optimized magnetic field, a highly accurate and precise planer and collinear arrangement of the coils. 2-DOF magnetic actuator manipulation system were designed and developed. Moreover, using a 2-DOF magnetic actuator system, a magnetic micro-robotic manipulation system with visual feedback was designed and developed. Fe_3O_4 iceberg like microstructure and The motion of Fe_3O_4 base particles on microrobots is studied using an open-loop control system (with visual feedback). Microbots show rotating, and linear motion of the micro-robot in ROI show the capability and movement controllability of the system.

Key Words: *Magnetic Actuation, visual feedback, micro-robotics, optimization, motion control*

Table of Contents

Declaration	i
Language Correctness Certificate.....	ii
Acknowledgments.....	iv
Abstract	vi
List of Figures	ix
List of Tables.....	xi
CHAPTER 1. INTRODUCTION.....	1
1.1 Background, Scope, and Motivation	2
1.2 What is a Microrobot?.....	3
1.2.1 Application of Microrobots and actuation	3
1.3 Research objectives.....	5
Conclusion.....	6
CHAPTER 2. LITERATURE REVIEW.....	7
2.1 Micro Robotics	7
2.2 Micro Robotics Actuation Techniques.....	9
2.2.1 Actuation with a single source.....	9
2.2.2 Hybrid Actuation System.....	12
2.1 Overview of Magnetic Actuation System	13
2.1.1 Single permanent magnets systems.....	13
2.1.2 Multiple permanent magnets-based systems.....	15
2.1.3 paired Electromagnetic coils-based system	16
2.1.4 The system with distributed Electromagnetic coils	17
Conclusion.....	19
CHAPTER 3. DESIGN AND DEVELOPMENT OF ELECTROMAGNETIC COILS	20
3.1 Theory of Electromagnetic Actuation	20
3.2 Design and Development of electromagnetic coils	23
3.3 Magnetic field characterization of the Coils	24
3.3.1 Experimental setup for the coil characterization.....	24
3.3.2 Experimental Results	25
Conclusion.....	28
CHAPTER 4. DESIGN AND DEVELOPMENT OF 2-DOF MAGNETIC MANIPULATION SYSTEM.....	29
4.1 Design and development of Magnetic system.....	30
4.1.1 Impact of core.....	32
4.2 Magnetic Field characterization of the developed systems	33
4.2.1 Magnetic Field Characterization System	33
4.2.2 Single Coil Excitation and Magnetic Field measurement.....	35
4.2.3 Simultaneous Excitation of four coils and Magnetic Field Characterization.....	36

4.3	Micro Robotic Manipulation System	39
4.4	Motion control of magnetic microrobots.....	41
4.5	Magnetic Microrobots.....	45
	Conclusion	46
CHAPTER 5. EXPERIMENTAL RESULTS AND DISCUSSIONS		47
5.1	Experimental Results	47
5.1.1	Rotational Motion	47
5.1.2	Linear motion.....	48
	Conclusion	50
CONCLUSION		51
REFERENCES		52

List of Figures

Figure 1.1 Micro Robotics is the combination of Micro Technology and Robotics.	3
Figure 1.2 (A) Some actuation techniques used for the microrobot actuation (B) micro rocket actuated by chemically powered (C) helical nano swimmer magnetically actuated (D) nanowire motor actuated by Acoustic propulsion (E) sperm hybrid robot propel by biological actuation (F) microrobots different biomedical applications (G) For cargo delivery magnetically helical microrobot (H) microgripper with high precision for surgery (I) For a cancer cell to sense and isolate microrobot (J) for detoxification coated nanorobot [5].	4
Figure 1.3 Micro-/nano robots actuation localization, Functionalization, Design applications [6]	5
Figure 2.1 System with single permanent magnet [50].	14
Figure 2.2 The system with multiple permanent magnets [50].	15
Figure 2.3 System with paired Electromagnetic coils [37].	17
Figure 2.4 System with distributed Electromagnetic coils [50].	19
Figure 3.1 Step (I) CAD design spinal . Step(II) Developed coil after winding.	23
Figure 3.2 Different coils are developed for the design optimization.	24
Figure 3.3 Experimental setup for the coils to test the coils parameter such as length, current, and distance from the central axis of coils.	25
Figure 3.4 Electromagnetics coils shown dipole magnet on energizing by apply current.	25
Figure 3.5 graph between the coil length 'l' (mm) of the coil and magnetic field(mT).....	26
Figure 3.6 The graph between distance(mm) from the central axis of the coil and magnetic field (mT)	26
Figure 3.7 (a) Measured 'B' along X-axis and Y-axis on a plan at distance 'R' = 10 mm from the coil, Centre of the longitudinal axis Centre of the core is taken as the origin (b) Measurement scheme of magnetic field on a plan at distance 'R' from the Centre of the core.	27
Figure 3.8 The graph between the applied current and the magnetic field	27
Figure 4.1 (A) and (B)The Helmholtz,(C) and (D) Maxwell, and their generated field [4].	29
Figure 4.2 Step(I) developed electromagnetic coil. Step(II) CAD design of assembly holder step (III) developed coils are mounted on the 3D printed coil holder.	30
Figure 4.4 (a) A comparison of different permeability (b) hysteresis loop and for the magnet cycle [72].	32
Figure 4.5 Experimental setup to observe the field effects in the workspace in this setup Gaussmeter meter probe is mounted on the XYZ stage.	34
Figure 4.6 Measurement scheme in which schematic of coils, ROI center, and ferrite core base rod for measuring the magnetic field of the developed systems.	34
Figure 4.7 Measurement of the magnetic field along +X- and +Y-axis when moving tip of tesla meter from the center of ROI toward the coil with a motion resolution of 2 mm where its current value was set as 1.5 A.	35
Figure 4.8 Visual representation of the measured data on XY-plane.....	36
Figure 4.9 (a) Quadrant pole configuration when - X and - Y are internally south and X and Y are North from internally. (b) when X and Y are south internally and -X and - Y are North. (c) when all are north inside.	37
Figure 4.10 (a) Measured values for configuration (a). (b) Measured values for configuration (b). (c) Measured values for configuration (c)	38
Figure 4.11 Same poles facing inwards	39
Figure 4.12 Collinear Coils facing opposite poles	39
Figure 4.13 Schematic diagram of the system which is consists of DAQ(6259), XY stage for the motion of workspace, pc, and 2D coil system.	40
Figure 4.14 Complete magnetic micro-robotics System for the 2D motion of microrobot.	40
Figure 4.15 Electrical circuit diagram to control the 2D motion of the microrobot system.	41
Figure 4.16 Acting forces on the microrobot. F_m is a magnetic force, F_d drag force acting in a fluidic environment, and F_g is the gravitational force.	44
Figure 4.17 (a) Magnetic powder for the magnetite (Fe_3O_4). (b) Iron particles collected after laser cutter machine we use these particles as microrobot in our experiment	45
Figure 4.18 Hysteresis loop for the iron and the magnetite [73].	45
Figure 5.1 Trembling motion of Micro robotic Iceberg around 90 deg using variable DC magnetic field.	48
Figure 5.2: X-axis manipulation by using (-) x-axis coil.	49

Figure 5.3 Microrobot motion around the *Y-axis* by using the *Y-axis* coils.....49
Figure 5.4 Micro-robot of Fe_3O_4 particles motion around the *X-axis* by using *X-axis* coils.....50

List of Tables

Table 1.1 Sensing, Actuation, Control, and fabrication.	5
Table 2.1 Currently available types of actuation systems are their power mechanism, strength, present challenges, and opportunities [40].	11
Table 2.2 Type of hybrid Actuation their advantages and remarks.	13
Table 3.1: Wire length, Resistance of each coil, and length of the coil shown in figure 3.2.	24
Table 4.1 Specifications of developed prototypes.	31
Table 4.2 Magnetic field by energizing one by one and then energizing.	38

CHAPTER 1. INTRODUCTION

Latest developments in micro-electromechanical systems (MEMS) technology have enabled the fabrication of mechanical structures that are only microns or even nanometers in size with various functionalities, such as actuation and sensing. With these functionalities at such a small size, these structures enable many newly emerging applications in electronics, microfluidics, and biomedicine. While most such micro-devices are designed to work without mobility, with one exception – untethered micro-robots, can move inside a designated workspace to perform various tasks that cannot be achieved by others. . Because of their high mobility and small size, these micro-robots could potentially be ideal for healthcare applications such as micro-surgery and targeted medicine.

While many existing micro-robots can operate in both air and liquid, many of their potential applications are in liquid environments, such as inside the human body. In addition, fluids not only provide strong damping to slow the motion of micro-robots slowing their mobility compared to air, but they also reduce the effects of stiffness and adhesion, which together with the actual impact of robot motion. Make timing control easier and more reliable. Therefore, most of the research effort has been devoted to making micro-robots capable of performing various tasks inside liquids.

When a micro-robot moves in a viscous liquid environment, it not only experiences resistive drag force and torque from the surrounding liquid, but, in turn, it also perturbs the liquid by its motion, either in an otherwise fluid liquid. The flow in matter creates or replaces existing flows near the robot's body from its original pattern. The flows generated by the micro-robot are highly correlated with the speed of the robot, and it is, therefore, possible to locally manipulate the flow around the micro-robot by controlling its motion. For example, an interaction between the robot's motion and the surrounding fluid could provide thrust for micro-robots equipped with propellers specially designed to translate inside the liquid.

In addition, these interactions can affect objects visible inside the turbulent flow region. Therefore, the overall functionality of the micro-robot can be enhanced by improving the ability of the micro-robot to interact with the liquid environment in a controlled manner to perform various tasks. While recent advances in related research have begun to explore the use of locally induced flow from robotic motion for object-manipulation and three-dimensional (3D)

propulsion, the underlying physics is as well as microfluidic and biomedical applications. Mechanisms based on a more comprehensive understanding of Microfluidic and biomedical applications based on the underlying physics as well as mechanisms have not yet been developed.

Among the various speeds a micro-robot can achieve, we are particularly interested in rotational motion because it is simple to implement yet interesting. From both functionalities and fluid mechanics points of view. This thesis deals with understanding the interactions between the micro-robot and the rotational motions of the surrounding Newtonian fluid and the basis of such understanding is micro-object manipulation, 3D micro-robot propulsion, and biomedical and microfluidic applications such as particle sorting. Different types of microrobots reported in literature such bio-inspired, Helical shaped, micro sphere etc. Our main on magnetics micro spherical robots.

1.1 Background, Scope, and Motivation

In the past few decades, the financial cost and complexity of medical procedures have been increasing as USA healthcare per capita increase from \$788 in 1960 to \$12,110 in 2020 [1]. Patients' comfort can be increase while minimizing the turnaround, patient recovery, and the impact of a medical procedure time and cost reduction. Micro robotics can be very useful in minimizing the insidious footprint of the doctors, it also allows for more precise intervention [2].

However, vital organs of the body such as the heart, brain, spinal column, remain difficult to reach as well as a cell level such as cell manipulation, targeted drug delivery, and cell therapy were difficult before micro/nanorobotics. An emerging field of robotics from the last decades is magnetic micro-robotics to create microrobots. Which are easily accessible and helpful in the operation of unaccustomed or difficult to reach areas in particular for disrupting medical, bioengineering, manufacturing, ecological remedial, as well as in other prospective submissions [3]. Long-range, efficient, accurate, quick, and vigorous actuation methods and self-management of microrobots are typically enabled by a magnetic field. For the actuation of microrobot different actuation techniques are available such as chemical actuation, bio hybrid actuation and magnetic actuation. In this thesis our main focus about the magnetic micro actuator.

1.2 What is a Microrobot?

Micro robotics is the combination of microtechnology and robotics. Presently, in daily life, “Microtechnology” is used for various devices and systems as define in figure 1.1. For example, energy resources, automobiles, environmental supervising, mechanization, cameras, computer peripheries, printers, bio-medical treatments. These amusements enhance their precision, performance, and to make better their cost execution, energy consumption, and so on Microrobot is a tiny robot that is built to do specific tasks [4].

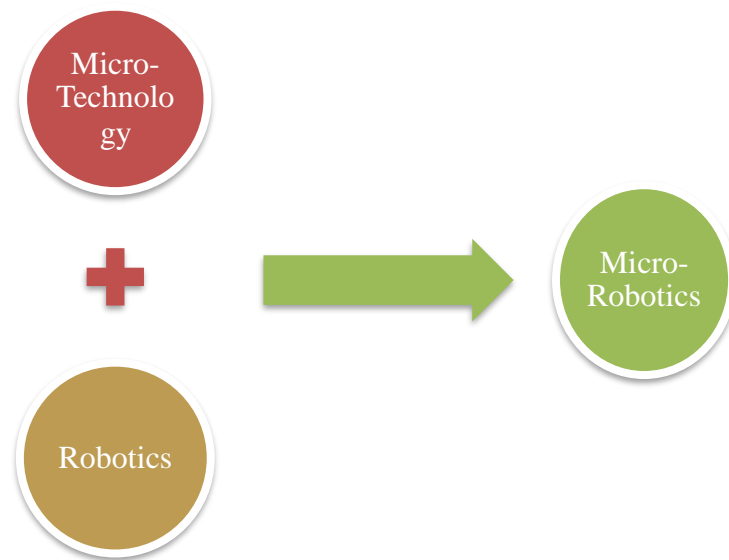


Figure 0.1 Micro Robotics is the combination of Micro Technology and Robotics.

1.2.1 Application of Microrobots and actuation

Robots is a machine able to do a complex series of tasks automatically and reprogrammable by the help of a computer. The main component of the robot is the controller(which work like a brain), mechanical parts (like a motor, wheel, gears, and gripper), sensor (which help the robot to identify the environment), power system (which help make possible to do a task) and the additional can be software and intelligence. The microrobot can be defined as a robot that either can be micro in size, or it can be capable to do a task at the micro-level. Size comparison between macro, micro, and nanorobots. These challenges are related to different applications such as miniaturization limitations on board trigger, powering, perceiving interaction, data processing, and implementation-specific functionality.

Two major approaches have been suggested in the scientific literature review for resolving these challenges such as an outside physical compel driven and the self-driven (utilizing self-generated gradients or components and deformities) microrobots. An outside source of energy is necessary for both strategies.it is very difficult to create microrobots at a micrometer scale with internal energy storage.

In characteristic methods, the magnetic field, optical, electrical fields, the acoustic, and the combination of those are involved but the local chemical environment can be used as an energy source in the future. Mostly in micro-robotics energy is delivered in the magnetic field by using these approaches. Most used for actuation methods magnetic fields are widely used in microrobot actuation approaches. Application-to-application of Microrobots in the bio-medical field, targeted drug delivery, surgery, sensing, and detoxifications as shown in figure 1.2.

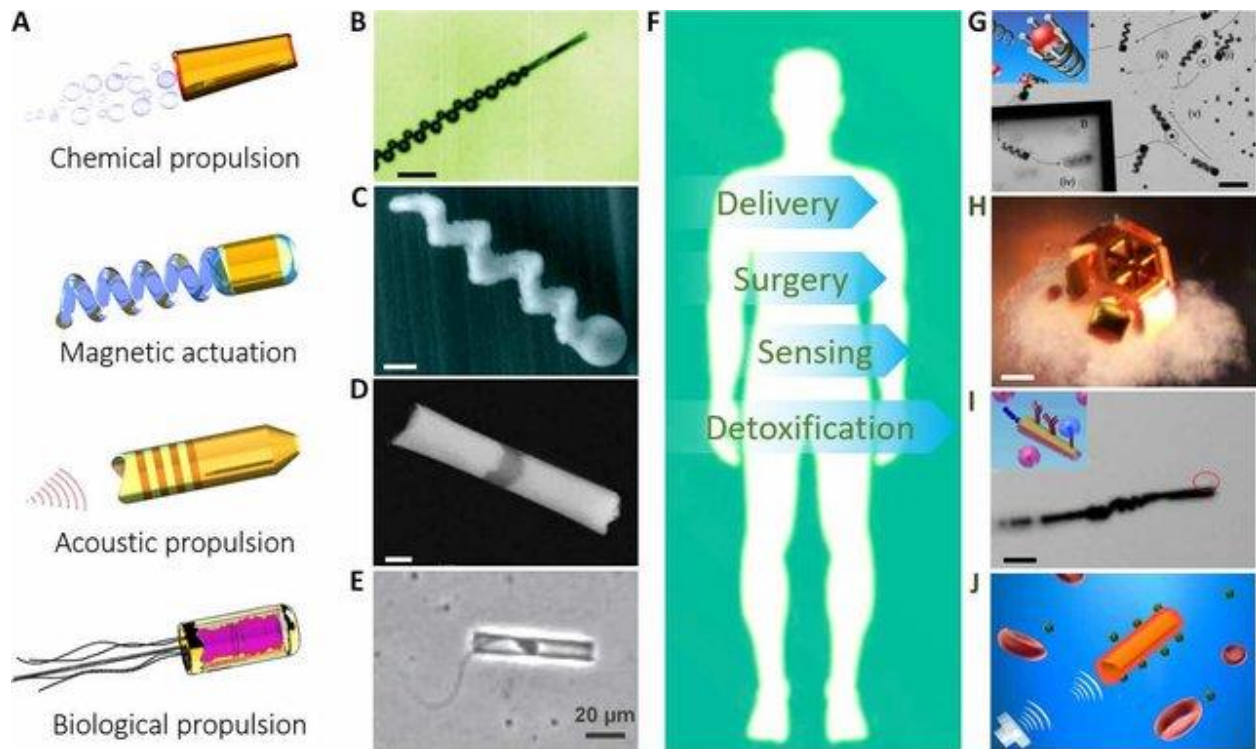


Figure 0.2 (A) Some actuation techniques used for the microrobot actuation (B) micro rocket actuated by chemically powered (C) helical nano swimmer magnetically actuated (D) nanowire motor actuated by Acoustic propulsion (E) sperm hybrid robot propel by biological actuation (F) microrobots different biomedical applications (G) For cargo delivery magnetically helical microrobot (H) microgripper with high precision for surgery (I) For a cancer cell to sense and isolate microrobot (J) for detoxification coated nanorobot [5].

Table 0.1 Sensing, Actuation, Control, and fabrication.

Sensing	Actuation/power	Control	Fabrication
Optical	Magnetic actuation	Magnetic force	Standard micro robot fabrication methods
Electron microscopy	Optical Actuation	Electric field	Polymer lithography
AFM	Piezoelectric	Atomic Force	AFM based nano manufacturing
TEM & Radioactive/ Fluorescence makers	Electrochemical/ bioelectrochemical	Electrochemical force	Milling and Micromachining
Ultrasonic	Electric field/ Electrophoresis / Di electrophoresis	Electric force	

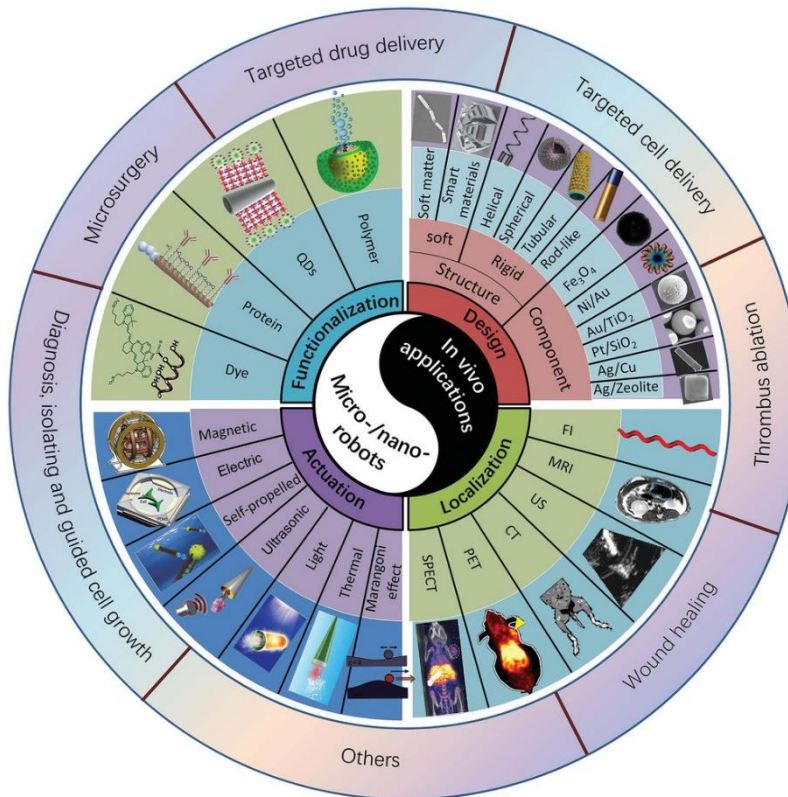


Figure 0.3 Micro-/nano robots actuation localization, Functionalization, Design applications [6]

1.3 Research objectives

- I. Design and development of electromagnetic coils and optimize parameters of electromagnetic coils
- II. Design and development of a 2-DOF magnetic micro-robotic system
- III. Motion control of micro-robot through visual feedback

Conclusion

Micro robotics is the combination of micro technology and robotics. Applications such as targeted drug delivery, targeted cell delivery, cell-targeted delivery, thrombus ambulation. Wound heling, microsurgery, cell graded growth, and others.

CHAPTER 2. LITERATURE REVIEW

2.1 Micro Robotics

Due to the small scale of the microrobot in dimensions, as shown in figure 2.1. they have accessibility to tiny and complicated environments where any other microrobot and humans are hard to reach [7].

Controllable, released and their mobilizability of microrobots make them eligible for various applications, including everything from industrial tasks to in vitro and in vivo tasks. For example, industrial tasks that are enabled the micro-assembly for microrobots by micro-transporting, micromanipulation, and sorting of micro-objects [8]. In applications like cell surgery, Microrobots are helpful tools in dealing with biological cells, due to their high replication and high throughput. Microrobot can efficiently move, and sort cells can operate very effectively down towards a cellular or a sub-cellular size, in that way it can anticipate in vitro interaction [9].

In micro-electromechanical (MEMS) systems technology, and integration of the microfluidic chip and robotics make the greatest innovation in biomedicines [10]. In the microfluidic chip, the microrobot can be load several objects as well as transport them to desirable places by the precise control of the movement with high-level thrust power, and the injecting system of motion[11].

For a wide variety of environmental applications, micro-robots provide opportunities, like environment sensing, monitoring, and remediation [12]. In minimally invasive surgery, mainly in-Vivo submissions of microrobot have been applied, for example, the targeted cell delivery, radiation therapy, hypothermia, material removal by a mechanical process, or acting like straightforward static structures [13]. Because microrobots have the dimension of only a few millimeters or less, so they can access certain places inside the human body would as wireless interference among them the blood circulatory system, urinary, and central nervous system.

The hard and soft magnetic material can be used for the formation of a micro-robotic body. commonly micropolitics is made up of hard magnetic material like NdFeB microparticles (SPIONS,) [15] superparamagnetic iron oxide nanoparticles (SPIONs), [16] CrO₂ ash, [17] FePt nanoparticulate, and another hard and soft nanoscale, the magnetic micro, discs wires, particles inserted inside or engaged on to the external surface of the body.

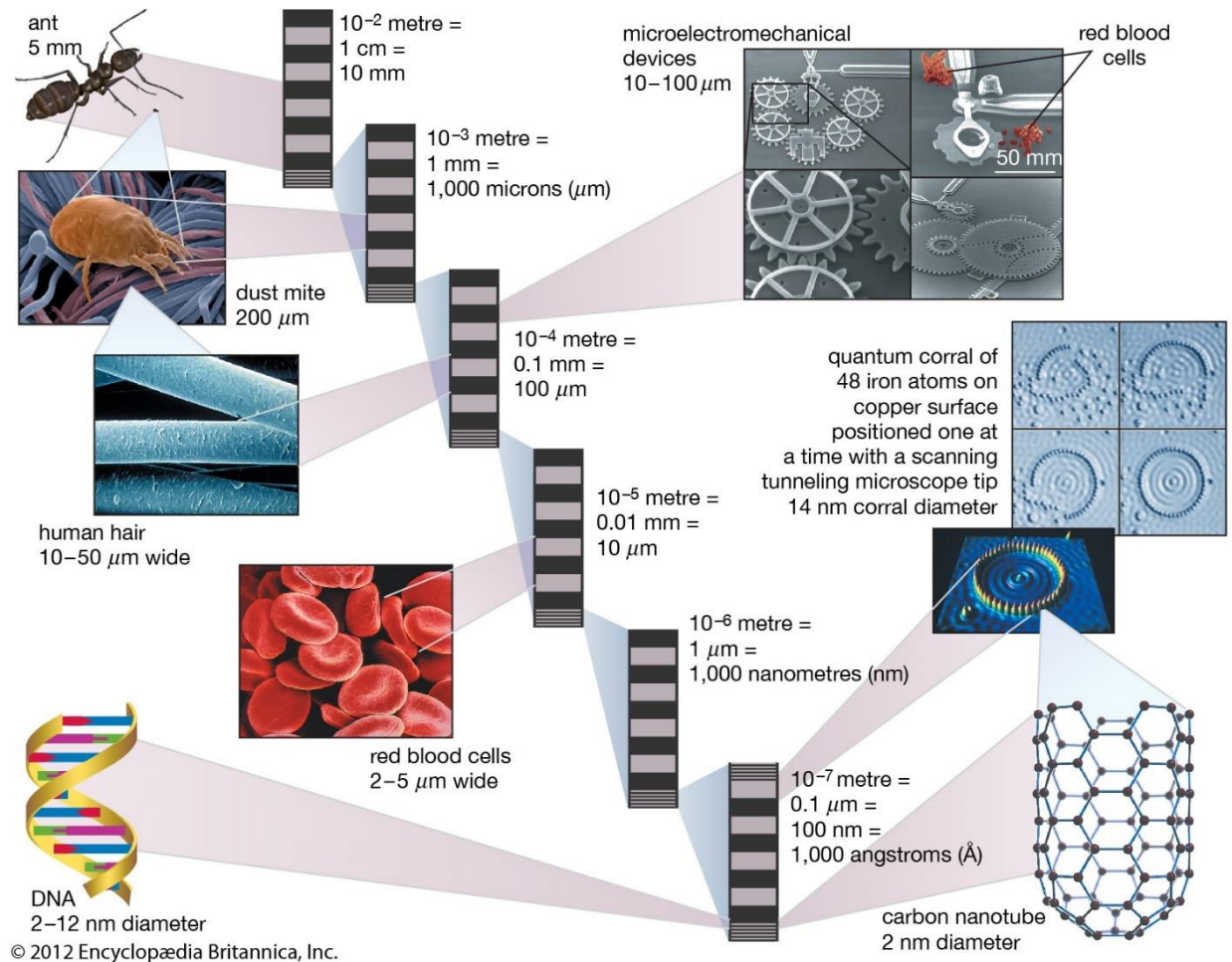


Figure 2.1 A comparison between Macro, Micro, and Nano objects [14].

Furthermore, other specific magnetic substances may also be splattered at a microrobot exterior like nickel and cobalt, etc. as a Nanofilm coating. The compatibility of micro-robots toward their operational environment is vital for a given particular application, micro robot material like one of the most required for medical applications will have to be bio-compatible to be able to use within the human body for the shorter-term and longer-term duration [18].

Additionally, an essential raw material obligation of the micro-robotic body under these application circumstances is called biodegradability. The condition that the microrobot could not be eliminated from the body spontaneously or through a catheter sort of medical equipment. The magnetic robots can make it easier to accomplish for either polymer material or the magnetic body part by using a wide variety of material, authorized by US nutrition and medication administration, magnetic microrobots biocompatibility and biodegradability can be used. Though, instead of the magnetic component, widely used in magnetic materials are not typically

biocompatible. Nevertheless, there is a need for medical devices, for safety regulations that is why magnetic robots should be biodegradable to carry out their activities within the human body. In this respect the best bio-compatible magnetic substance is SPIONS. They are more attractive compostable robots within the body. Yet, SPOINS are making the magnetic actuation feebler for microrobots with a dimension of only some micrometers due to weak magnetizing properties.

Fueling microrobots through built-in, the energy sources are presently difficult to accomplish. Hence, some off-board actuation methods are used. For example, the actuation of a microscale, particles in the die-electrophoresis forces in, piezoelectric actuation [27], electric fields [19], thermal actuation [20], powered electro-osmoregulation force [21], bacteria actuated [22] chemical and biological fuel-driven microrobots [23]. In for vivo applications the aforementioned methods face problems, in-vivo, for instance, piezoelectric actuation necessitates a high-level voltage, and bacterial actuation needs to maintain minimal cytotoxic effects. The electromagnetic system (torques and forces) can be useful for implementation without any distortion for in vivo applications. Various magnetic actuation techniques by enabling different dimensions working space and degrees of freedom have been used by researchers. Such as from open-loop control, [24] to closed-loop end-to-end placement control [25] either a closed-loop path tracking [26] , and a variety of motion control techniques.

2.2 Micro Robotics Actuation Techniques

Due to the small and reshaping quality of micro robots, they have lots of applications in medical and other fields. In submillimeter robots, due to restricted volume, it is extremely difficult to incorporate microrobots with the power supply, processor, and actuator conventional onboard components. For the control and actuation system various approaches have been used, single sources for example, magnetic, ultrasonic, optical, electrostatic, and chemical actuation [27] and also hybrid source such as chemical and magnetic, magnetic and ultrasonic and biohybrid.

2.2.1 Actuation with a single source

As technology is growing Acoustic fields is very emerging actuation system for off-board manipulations and propulsion. And it is a very power full gripping source for powering and motion in self-controlled directions microrobot. But its application and purposeful design are

currently insufficient in biological use and require maximum effort work future advancements. Acoustic streaming and acoustic radiation force are the physical effects of acoustic fields which are frequently discouraged. A standing wave can generate Acoustic radiation in the form of force. in a biologically safe way resonator, which is used for the back and forth of reflection of a sound wave. This helps to create a hydrodynamic drag force for a microrobot in a fluidic environment that applies a driving force of the sound on antinodes and nodes, which are called highest and lowest and amplitude points, correspondingly [28]. In this actuation system, the wave function is applied on corresponding the direction of motion of the microrobot. In this way, this approach could be extremely effective in influencing the worldwide movement of many microrobots to convey them within the targeted place. this method is specially used in applications like tissue engineering particularly, for the method of tempting to arrange the cells in 2-dimensional and 3-dimensional patterns as complex groups [29]. Acoustic fields do not have discrimination manipulations of the microrobot, so it does not need a special structure or a special material. However, recently oscillatory fashion as the relevant application of acoustic radiation energy fields has been launched for choosy addressability. To generate enough thrust Micro-swimmer bodies are trapped oscillating bubbles [30].

In thermal actuation, an air-liquid boundary will stimulate, and fluid stream from the color area to the hotter areas, owing to the nature of surface tension which is temperature-dependent. In the temperature gradient, manipulation is caused by concentrated light illumination. The micro-swimmers (micro-bubble) are controlled because they are held by the air-liquid. The light is demonstrated only in 2D, and it is needed that required special steps that transduced the light in heat are a major drawback.

Recently a huge number of foams are produced and they are moved autonomously by utilizing liquid-crystal devices [31]. Microrobots are trapped into bubbles and then push to word the desired site [32]. Among all these actuation methods, magnetic actuation is preferred over any other actuation system due to its safe transparent, and controllability [33]. For microrobots, magnetic actuation encouraged even the design is onboard or offboard the synchronized detection of active sense modality and micro size is very good [34]. That is why magnetic microrobots have been widely developed and reported [27].

Magnetics manipulations are firstly used by ancient Indians to attract the foreign bodies beneath their skins by using lodestone might be the earliest example [35]. In the 1920s the Germans firstly demonstrate the magnetic method in biology, they used an electromagnetic field to observe the viscosity of protoplasts[36].

Magnetic field is very necessary to develop the reliable and proper actuation system, to improve clinical and scientific outcomes of magnetic microrobots. Magnetics field can be generated by permanent magnet and electromagnet. Numerous of magnetics systems have been developed. Such sys produce 2,3 and multiple degrees of freedom magnetic field [37]. Some of them can produce magnetic gradients which can produce force for propulsion [38].

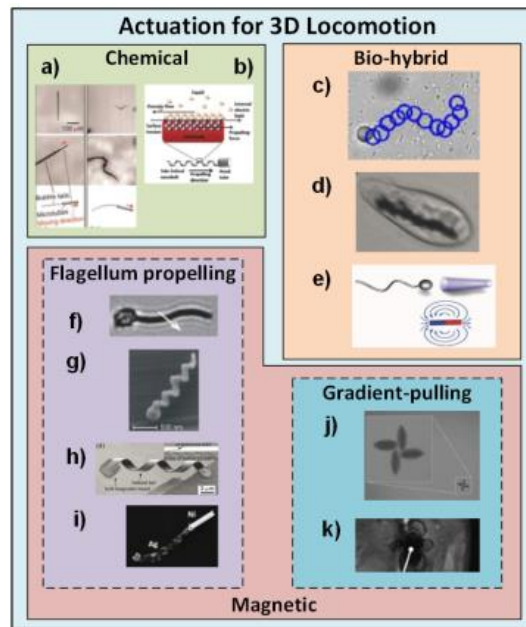





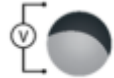


Figure 2.3 a) Microtubular b) Electro-osmotic swimmer. c) Bacteria propelled microbeads. d) Artificially magnetoacoustics bacteria. e) Sperm-flagella driven micro-bio-robot. f) Flexible artificial swimmer. g) Helical propeller. h) Helical artificial flagella. I) Flexible propeller. j) Nickel micro-robot is driven by the OctoMag system in 3D. k) MRI-powered and imaged magnetic bead. Figures are reprinted from the references accordingly [39].

Table 0.1 Currently available types of actuation systems are their power mechanism, strength, present challenges, and opportunities [40].

Energy Source	Strengths	Challenges	Opportunities

Internals powered	Chemical 	Strong mixing, Chemotaxis, climbable, Self-governing motion, and Collective performance.	Have short life spans, can change chemicals environment, uncontrollable required toxic fuel.	Autonomy Drug delivery, environmental remediation, microscale mixing.
	Biohybrid 	Scalable, sensing capabilities, and energetic autonomy.	Limited operations to the biocompatible environment, minor volumes add to tasks based on synthesis particle.	
External powered	Magnetic 	Well-disciplined, fuel-free, and precise localization.	Limited workspace, high-cost equipment, and complex, slow speed, not autonomous.	Controls Drug delivery, preconcentration, microsurgeries.
	Ultrasound 	Preconcentration, strong, collective motion, and fuel-free.	Restrict by material selection, chamber geometry, and not autonomous.	
	Light 	Collective behavior, phototaxis, swarming, and controllable movement.	Due to medium characteristics and light penetration limited power and speed	
	Electrical 	Fuel-free, swarming, and controllable movement.	Due to chambers geometry restricted in low concentration environment	

2.2.2 Hybrid Actuation System

Use an actuation system with an internal energy source is very useful for the task for example sovereign cargo transport and improve. An external actuation system can provide on-demand and changeable power for an extended period. Comparable to the latest developments in hybrid actuation for microrobots with double or multiple powering, which is useful for both kinds of internal or external power source into progression, developed to get rid of the limitations of the typical actuation system [41]. These are different combinations like chemical and magnetic actuation, these kinds of systems based on robots with head catalytic and a flexible magnetic or magnetizable material based. In these types of systems actuations can work sequential or parallel manner. For instance, the chemical actuation starts working for propagation as the fuel ended the external magnetic field triggered and start motion microrobot by an applied magnetic field [42].

Acoustic and chemical hybrid actuation system has been developed based on asymmetric bimetallic nanowires. Likewise, the chemical thrust and serve as the lonely supplier of actuation as soon as the fuel has exhausted and the ultrasound field may be used to monitor [43]. Also, the same design approach was used for light and chemical hybrid actuation [44]. Another combination has been developed based on magnetoacoustics-based actuation such as system-based micro-agent based on a micro-structure the composition of spiral structure tied to the concave structure of gold part [45]. These kinds of hybrid systems stemmed in fully with adjustable propulsion and teeming behavior. The utilize of a hybrid superpower source can offer forms of movement (for example the brake and the acceleration) and new opportunities that could be impossible by utilizing an individual type of actuation system. Other future hybrid systems should provide new opportunities for interaction in new surroundings and microscale motion.

Table 0.2 Type of hybrid Actuation their advantages and remarks.

Name hybrids Actuation	Advantages	Remarks
Chemical and magnetic actuation	This system can work sequential or parallel manner	These kinds of microrobots with head catalytic and a flexible magnetic
Acoustic and chemical actuation	Adjustment impact with further powerful	Density-reliant acoustic thrust
Light and chemical hybrid actuation	Faster due to photochemical reactions and high temperature-induced which is beneficial for the tumor	Limited by the reaction level and curved the geometric shape
Bio-hybrid	Effective and self-controlled motion	They show the diverse biomimetic collective behavior

2.1 Overview of Magnetic Actuation System

Numerous actuators were designed and developed for the accurate control of magnetic microrobots. Based on their configuration and magnet source these systems are divided into four categories.

2.1.1 Single permanent magnets systems

Applying magnetic force or torque via changing the position of a single permanent magnetic can control magnetic micro robotic either in translational or rotational motion, the use of single magnet has a very low price and high compactness. In this actuation system, magnetic field conducted by the handholding in the early remote actuation using single magnetic. A very intuitive and experienced operator is required to operate the kind of system. Ciuti et al. [46] in their systems as shown in figure 2.1(a) defined the control as the main reason resulting in high dependence. Moreover, long operating times and imagining are also challenges for operation.

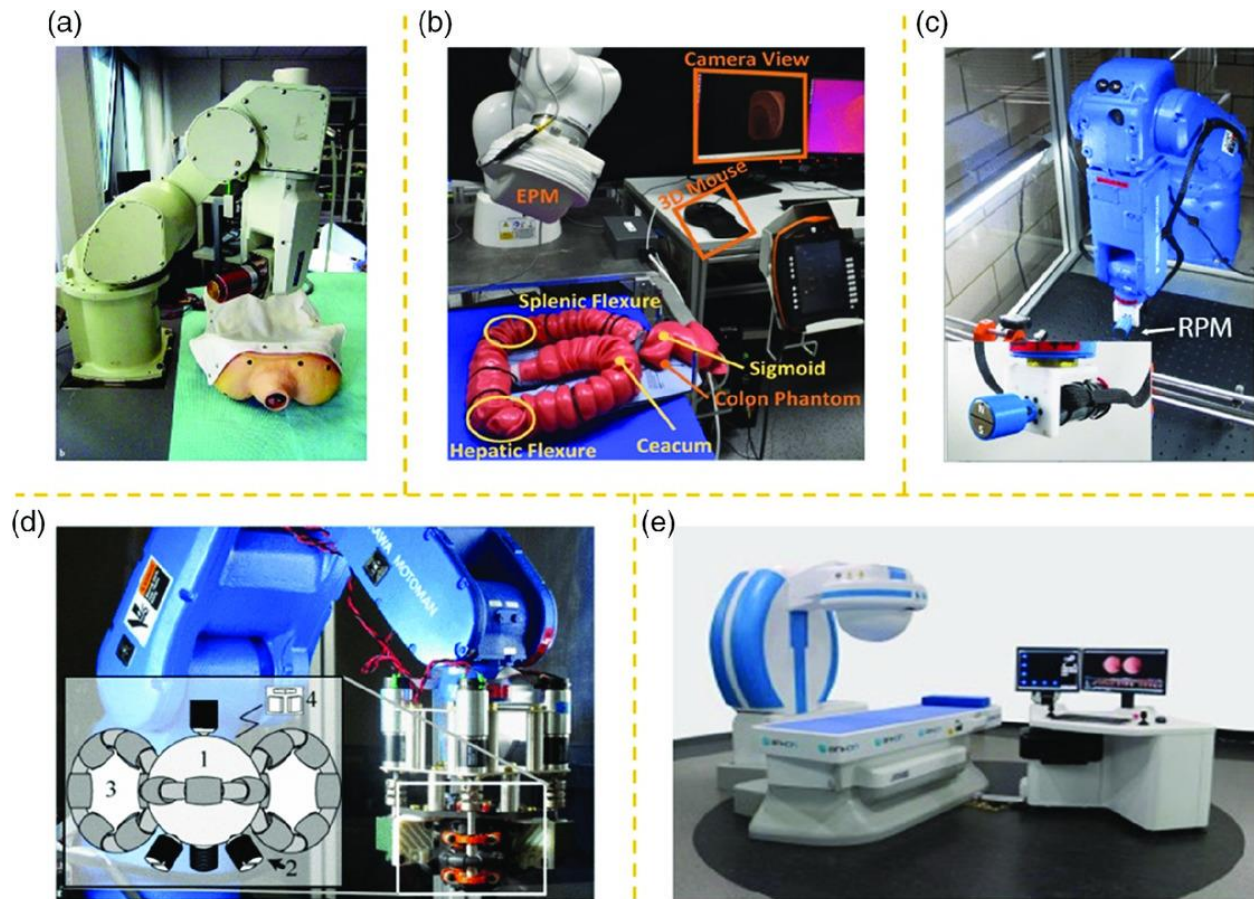


Figure 0.1 System with single permanent magnet [50].

Permanent cylindrical magnet by attaching them a six degrees of freedom industrial they utilized as robotics arm to accurately control to remote for overcoming this kind of drawbacks as shown in figure 2.1(b) [47]. Drag force controls the locomotion, and the torque movement is steered by the orientation of the magnetic device in this scheme. A virtual magnet link was designed to obtain an effective interaction between the controlled device and the permanent magnet. This makes robotic operations more reliable and precise labor-intensive operations can be obtained. Similarly, this kind of adopted commercial system of robotic manipulation was proposed by another group [48] as shown in figure 2.1(c).

Due to the constrained surface contact of these magnetic devices so these kinds of systems developed up to four degree of freedom for respective control system having two degrees of freedom orientation and two degree as freedom of locomotion. Another researcher team applies a similar configuration although a different control approach. With parameters such

as buoyancy, force magnetic force, and gravity. They developed and experiment with five degrees of freedom control in the open air-fluid environment [49] as shown in figure 2.1(d).

2.1.2 Multiple permanent magnets-based systems

System with multiple permanent magnets is developed for various purposes, the main is to produce high consistency for torque actuation. Niobe system design and developed by stereotaxis in 2003. The most famous one, now it is used in the treatment of cardiovascular diseases for guiding magnetic catheters. More than a hundred hospitals are using this system to treat more than a million patients. This system has two permanent magnets spread around the bed. Both magnets can rotate in tiltable housing [51] as shown in figure 2.2(a). It has very efficient orientation control because each magnet generates a gradient field.

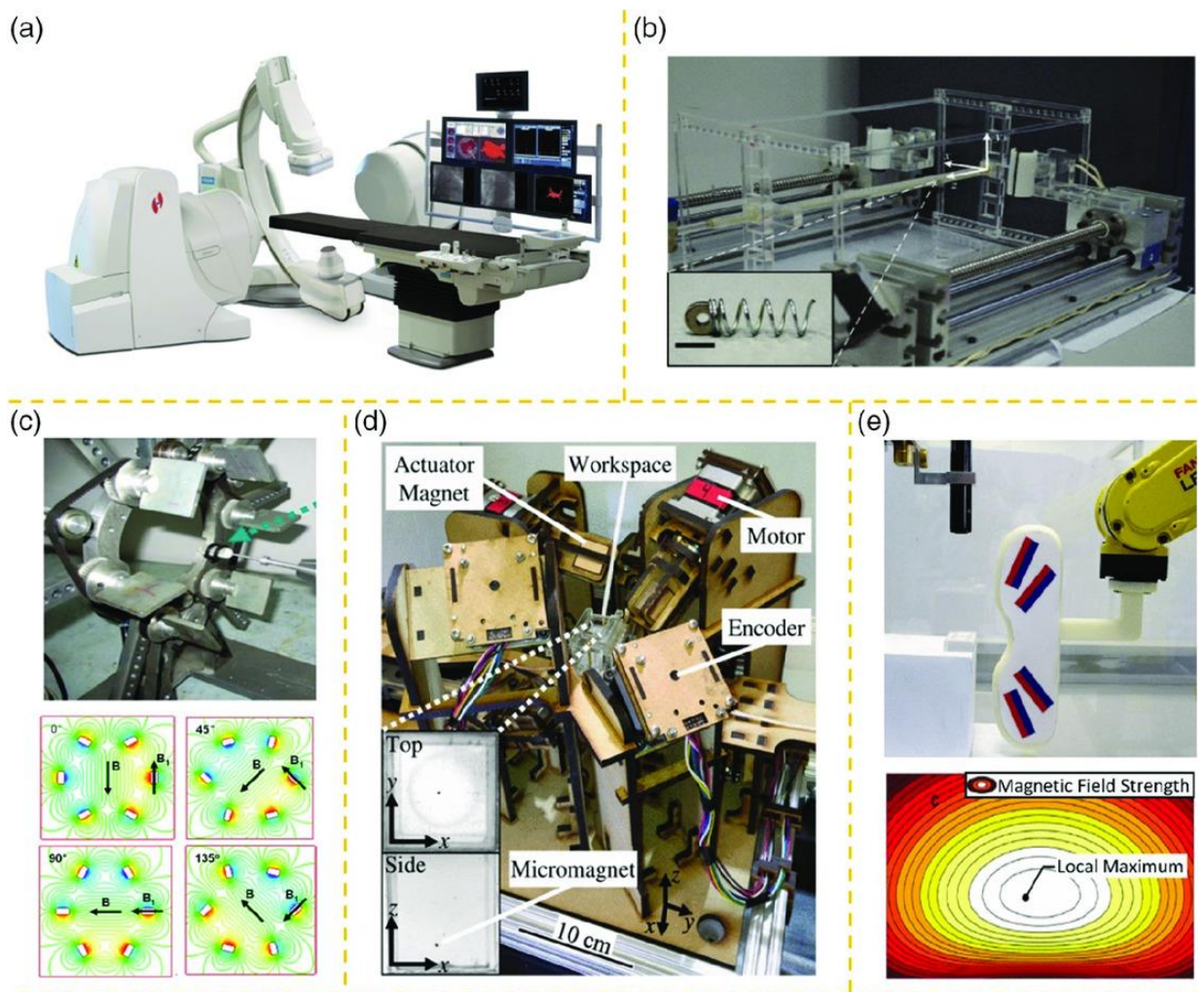


Figure 0.2 The system with multiple permanent magnets [50].

Stereotaxis upgrades his Niobe system and gave it name of Genesis system. Stereotaxis improves size, weight, and flexibility in movement. Genesis system consists of two rotatory magnets and two linear motion stages [52] as shown in figure 2.2(b).

System, all magnets are fitted with set angles and can be rotated by themselves using a strap-aligned system, producing a magnetic field that rotates right in the middle with the force of the side and the reverse. This system only detects the explosion of 1-DOF at present but are sufficient to ensure proper operation. The simplification of the system has achieved the usage of an everlasting magnetic range. By Ryan et al. a novel design is proposed and developed, which comprises eight impartial permanent magnets. Their of device can create an omnidirectional magnet field and a gradient of an area of diverse sizes [53] as illustrated in figure 3.2(e).

2.1.3 paired Electromagnetic coils-based system

In orthogonal distribution, a pair of coils refers to more than one electromagnet with clear, with the primary position around the workspace. These kinds of actuation systems use electromagnetic coils such as Maxwell, Helmholtz, and cylindrical coil. In this manner mostly Helmholtz coil with compositions of numerous Helmholtz coils, and around workspace each pair make the same moment perpendicularly. In this setup with the direct orthogonal decomposition of the magnetic field, the actuation system may produce unpredictable magnetic fields including excessive regularity into the plane an area two or three Helmholtz coils [54] as shown in figure 2.3(a).

By changing the current in an electromagnetic coil, the proliferation of magnetic fields can be produced, for example, because of rotational, fluctuating, tapering, and alternating magnetic fields. Biaxial square-shaped Helmholtz coils have been additionally evolved for different purposes, which include enlarging the ROI.

A coaxial system based on set of Maxwell coil and Helmholtz coil both constructed. This is system mounted on a rotating basis phase which can be spin about its central axis. Into this system, the Helmholtz coils and Maxwell coil are used to creating a uniform magnetic field and a uniform gradient respectively. These uniform field was responsible to produce rotation and propulsion [55] as shown in figure 2.3 (b). The propulsion force is preserved in parallel with a common axis, and the two-dimensional propulsion of the tool is performed utilizing rotation. In addition,

Jeong and his team perpendicularly use Helmholtz-Maxwell coils for three-dimensional motion [56] as shown in figure 2.3 (c). In this configuration of the system, the internal Maxwell and Helmholtz coil is static, and around the horizontal axis, an external Helmholtz and Maxwell coil can be rotated.

Yu and his team use two Maxwell coils and a three-axial Helmholtz coil [57] as shown in figure 2.3(d). A stationary Helmholtz is situated on the exterior of the z-pivot, and the opposite rotating Maxwell coil is spinning around the z-axis. The device can produce a high-frequency magnetic discipline and restrained-frequency spectrum gradient.

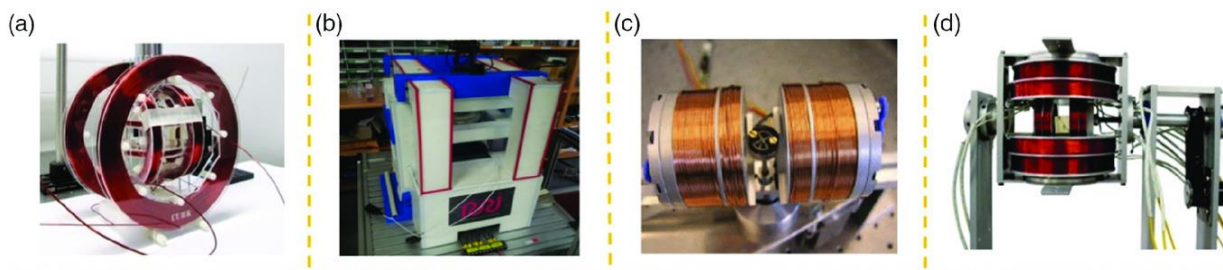


Figure 0.3 System with paired Electromagnetic coils [37].

2.1.4 The system with distributed Electromagnetic coils

Another branch of electromagnetic energy systems uses dispersed electromagnets designed to improve energy efficiency and reduce set limits. Most programs with paired coils tend to include a working area with electromagnet coils. On the other hand, distributed electromagnetic systems are typically composed of column coils that are rotated and oriented. In the meantime, it is best to install co-iron-cores a coil to focus and improve the magnetic field, which can be easily influenced using the outside magnetic field and power dissipation as soon as the magnetic field vanishes.

OctoMag is the first representation with the configuration of the same distributed components that detects five degrees of freedom wireless fraud. It possesses eight of the identical electromagnets separated into two pairs [58] as shown in figure 2.4(a). Each electromagnet was set as a 45° angle relative to the standard measuring axis. We define this angle as the active deviation. Deviation from the bottom set will be 90° . In addition, the higher array has a 45° spin down to next the normal measuring axis.

The following design considerations are designed to have adequate power control in all workplaces. Subsequently, the Mini-Mag was revamped beginning with OctoMag, its factors

selected for high integration [37] as shown in figure 2.4 (b). The planned subtraction of the two groups is 42.5° and 64° , respectively. Salman pours et al. suggested a system with eight electromagnetic coils, [59] as shown in figure 3.4(c). In such a system, four electromagnets on the internal set are a deviation of 59.5° , four rods on the outer set have a deviation of 90° , and a deviation of 45° .

The external electromagnet radiator is two times that of the interior. Son and his team improved magnetic field performance in a system that has nine electromagnets arranged on a 3×3 grid [60] as shown in figure 2.4(d). Design factors are adjusted to your prerequisite for both local and operational performance. Four electromagnets with zero deviation, four with a slight deviation, and an additional ninth electromagnet right in the middle will be utilized to stabilize the gradient field and magnetic field toward the normal direction. Electromagnets within the system are positioned on a side of the middle plane, i.e., the working surface installed inside. A notable characteristic is that those configurations are easy to be integrated with nature (such as OctoMag can be put on top when it is inserted into the skull, collar, and shoulder).

Unequal distributions are easy to integrate imaging techniques and other appliances. New strategy arranging the electromagnet throughout the working of magnetic field produced and the field gradient. its upper and lower sets are placed on either side of central to the plane [61] as shown in figure 3.6(e).

Each group consists of four electromagnetic coils at right angles the magnets with a 45° deviation, and a 45° probability present between these two sets. A different system with the same configuration, but the variation of both sets is 60° to increase the separation between and the independence of the electromagnet [62] as shown in figure 3.4(e). Additionally, there are other systems with a high set and a low set vertical set, and that means the malfunction is equal to zero. yog et al. designed a system with electromagnets set at the three-dimensional having space at 90° cornering each other. Eight system electromagnets are organized for each vertex of this cube and at every point in the middle [63] as shown in figure 2.4(f).

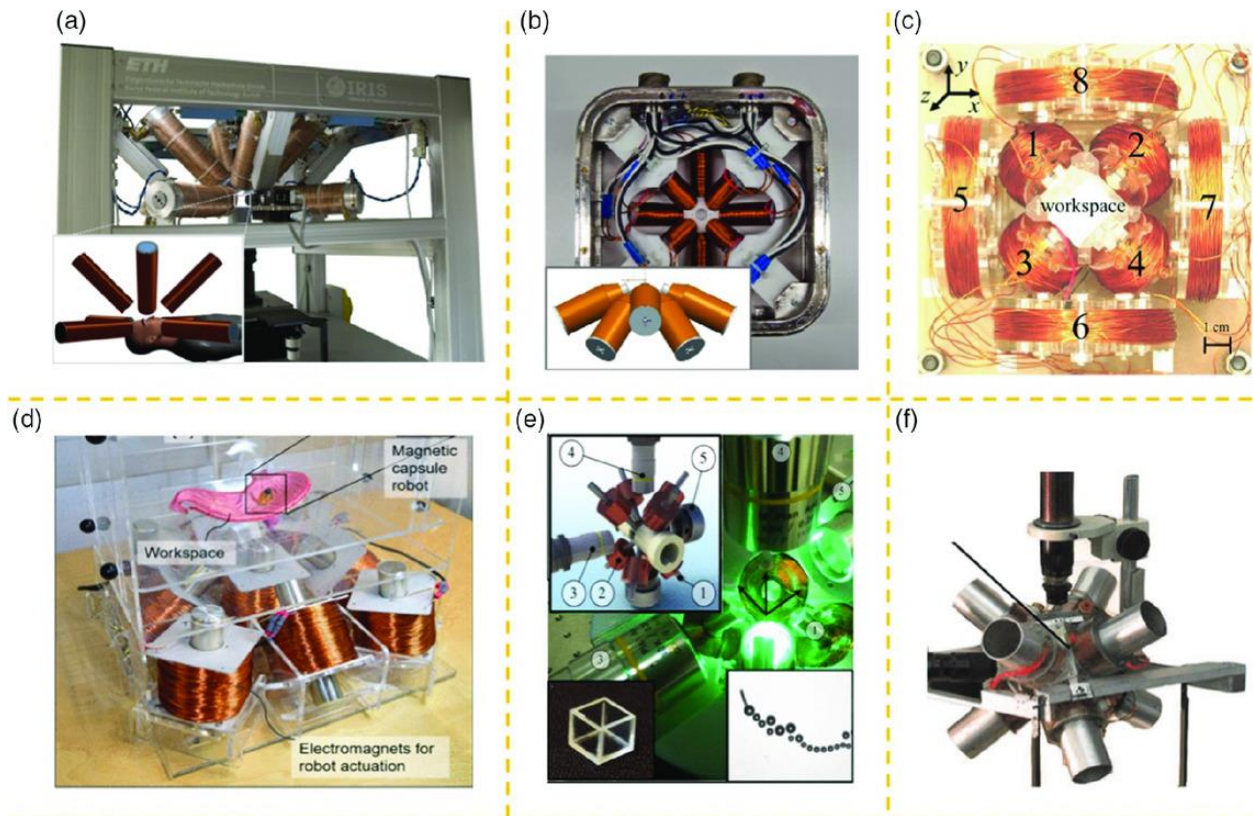


Figure 0.4 System with distributed Electromagnetic coils [50].

Conclusion

This chapter discusses the type of microactuators single source such as, chemical, biohybrid, and ultrasonic, and magnetic micro-robotic system etc. afterword we discussed hybrids systems such as magnetic and chemical systems, ultrasonic and magnetic systems. Later on we discuss the type of magnetic actuation such as single permanent magnet, multiple permanent magnets, paired electromagnetic coils.

CHAPTER 3. DESIGN AND DEVELOPMENT OF ELECTROMAGNETIC COILS

This chapter introduces magnetic actuation systems, their design, affecting parameters, and our coils design system, their parameters, and tests.

3.1 Theory of Electromagnetic Actuation

Magnetization and Volume, both properties of magnetic materials, are the most significant design factors from the magnetic actuation perspective. Where the material having the largest magnetization ability and highest volume has used the torque and magnetic forces concerning the microrobot.

In micro-robots, a very considerable point is how microrobots can make separate decisions for their actions? The microrobots are controlled externally by people and computers, which is the more traditional approach. A very interesting possibility that is based on the behavior of their neighboring robots or local environment is that of developing untethered microrobots that can make decisions autonomously. Magnetic microrobots can achieve their desired tasks to navigate in diverse environments by these applications such as the surface, submarine, and air-water boundary propulsion methods.

However, magnetic actuation at the size of tens or hundreds of micrometers works well for the microrobot. Accurate and high-level DoF control (usually five-degree of freedom management possible, which may be extended to six degrees of freedom control) [64] depending upon the microrobot magnetization uniformity, precise, and degree of freedom ability of the magnetic field generator. Numerous systems are available in the literature with six to eight degrees of freedom actuation mechanism by combining torque and force control [65]. The algorithm and configuration of the actuation system can help determine the ability of the magnetic field. Sometimes Actuation's systems are made up to create a special type of magnetic field, and effectors are used to maintain multiple modes. Arena of magnetic actuation depends on working scenarios of magnetic fields such as in vivo for medical treatment and in vitro micromanipulations cover only millimeters to tens of centimeters [66]. For the last few decades, microrobot is an emerging field that is another reason for developing magnetic actuation. Lots of

well-planned facilities had been developed as proof-of-concept prototypes on the stages. Magnetic actuation methods depending on different designs will be able to create greater speed motion and strength.

Motion range is restricted to the applied magnetic field into the arena. With the appropriate feedback control, the motion precision of the magnetic micro-robotic method could be high, depending on whether the locomotion precision and input stimulation. Magnetic microrobots cannot move and carry out any work with internal power they always require an external magnetic force control.

Magnetic actuation system needs a more massive and complex support actuation\ control apparatus to monitor the microrobot and the operation magnetic method needs comparable to the unified imaging methods, which is separate from the actuation technique for specific applications.

Through the magnetic actuation, multi-robot manipulation in the two-dimensional plane surface is attained. There are three ways localized selective trapping [67], heterogeneous microrobot design [68], and discriminatory magnetic immobilizing techniques. However, this type of magnetic field is not easily manageable for most applications and this magnetic field is used as the major drawback. The second approach is only feasible in such a condition that the robot responds to the electric magnetic field or gradient in different ways. even though such various microrobot designs, the approach is easy to implement is easy to apply, they are not made to control many other micro-robots while they make unique responses entirely independent from the rest.

The third approach uses a variety of magnetic materials with different magnetic hysteretic concurrently to attain the addressing magnetic control, in which different mixed magnetic substance-in in following the microrobots can be operated remotely converted to a nonmagnetic robotic body [69]. If the robot orientation can be control precisely then the method is measurable to many robots. This type of remote overpowers the need for additional pulsing electromagnetic coils. The pulsed electromagnetic coil may be applied to a rapid high field in the direction the robot is moving in three-dimensional space.

Magnetic actuation may penetrate deeply into the region of the person's body when an external magnetic source is switched off with the computer or human interference then the robot would completely halt in the magnetic actuation method. For example, in the case of auto-driven

biohybrid or as a catalyst for micro-swimmers, micro-robotics are constantly dependent on external power sources and cannot be auto-propelled individually. If an external power source is switched off, then a robot can be completely halted in the unlikely event of an emergency, so this property of robots is extremely beneficial for secure applications.

Another perception was that of developing microrobots that complete their tasks without any external power. Polymers are sensitive according to their environment so this sensitivity of polymers can also use to develop robots that are based on thermal gradient [70]. The next different line of thought about future awareness of microscopic robots that carries out the simple tasks without self –assemble or human intervention into a more difficult thing.

Magnetics actuation is achieved by applying magnetic force or magnetic torque on magnetizable objects or magnetic objects. Manufacturing an actuator with optimized parameters is of permanent importance for magnetic micro-robotic. Magnetic coils will be used to create a magnetic field by surroundings the workspace. Different parameters of the actuator impact the generated magnetic field such as length of the electromagnetic coil, and distance from the measurement point, and the number of turns.

The relation the magnetic field with different design parameters and variables is given by

$$B = \mu_r \mu_0 \frac{Ni}{l} \quad (0.1)$$

In equation (1.1) B is the magnetic field, N is the number of turns, i is the current flowing through the electromagnetic coils, l is the length of the electromagnetic coil, μ_0 permeability of air and μ_r permeability of free space. In this equation, N and l are the main design parameters.

Similarly, the strength of the magnetic field at a point is given by Boit-Savrat law as [71].

$$B = \mu_r \mu_0 \frac{Ni}{2\pi r^2} \quad (0.2)$$

The equation (1.2) is for only one loop, B is the magnetic field, μ_0 is the permeability of free space, N is the number of turns, and “ r ” is the distance away from the line segment to such an extent of interest.

$$B = \mu_r \mu_0 \int_{wire} \frac{Id\vec{l} \times r}{r^2} \quad (0.3)$$

This equation is for the number of all loops of wire around the bobbin.

3.2 Design and Development of electromagnetic coils

As we discussed in early sections magnetics systems based on magnetic actuators and numerous actuators were designed and developed for the accurate control of magnetic microrobots. Based on their configuration characteristics and magnetic source these systems are divided into four categories. Magnetic actuation systems can divide into categories system with permanent magnets and electromagnetics coils based magnetic actuation systems and then divided on the bases of configurations single permanent magnet, multiple permanent, paired of electromagnetic coils, and distributed electromagnetic coils-based actuation system. For our experiments we chose paired coils because the coils are easy to control. Best for the 2D magnetic systems easy to design and develop.

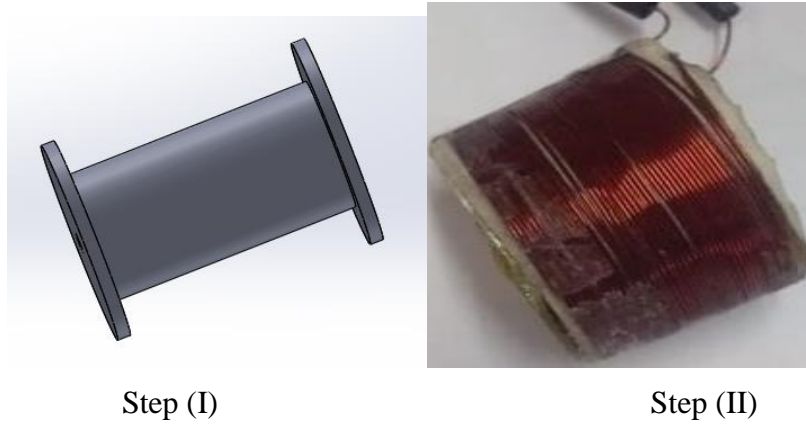


Figure 0.1 Step (I) CAD design of a cylindrical coil. Step (II) Developed coil after winding.

There are three main types of paired coils such as Maxwell, Helmholtz, and cylindrical coils. For this experiment, we chose to design cylindrical coils because they are easy to design and develop. Magnetic actuators of different lengths were fabricated with different parameters. Their parameters are given in table 3.1 and shown in figure 3.2. For the design optimization, we did different experiments which are given below in schematic shown in figure 3.6.

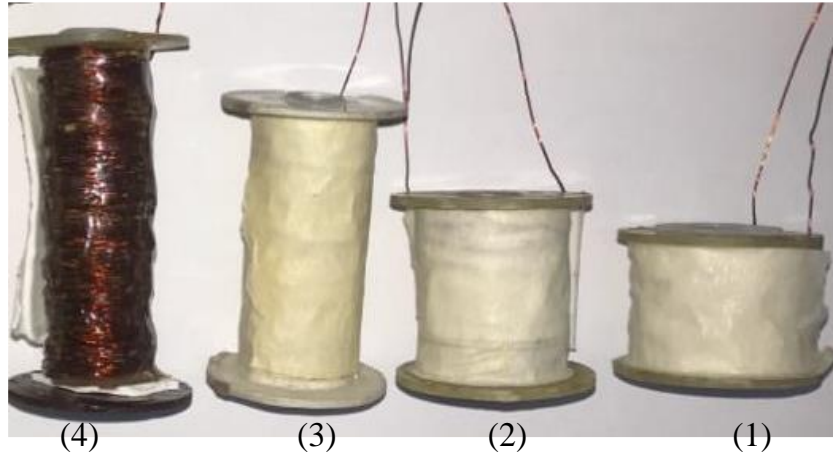


Figure 0.2 Different coils are developed for the design optimization

Table 0.1: Wire length, Resistance of each coil, and length of the coil shown in figure 3.2.

Prototypes	Coil length (mm)	Resistance (Ω)	Wire length (m)	Wire diameter (mm)	Core	
					Length (mm)	Diameter (mm)
1	26.50	7.7	40	0.43	26.50	8.5
2	34	7.7	40	0.43	34	8.5
3	54	7.7	40	0.43	54	8.5
4	66.50	7.5	40	0.43	66.50	8.5

3.3 Magnetic field characterization of the Coils

Although tremendous research is available on the design parameters of the magnetic actuators, however, it needs consolidated research on the topic so that the process will be optimized. In this thesis, we investigate different parameters that impact the magnetic field generated by a coil.

3.3.1 Experimental setup for the coil characterization

The Custom-made experimental setup for coils design optimization is shown in figure 3.6 which is consists of a base plate with the XYZ stage with the resolution of 10-micrometer travel distance of 25mm. A probe of the gaussmeter (HT201) with a resolution of 0.1mT was installed on the XYZ micro stage, to accurately replacing a probe to gauge the magnetic field at a varying distance from the electromagnetic coil. A DC power source (REGOL DP 830 programmable power supply) has been used to simulate the electromagnetic coils. A probe has been placed at a

right angle to the main axis of the coil to gauge the magnetic field quite accurately. The manufactured electromagnetic coils were positioned on the 3D embossed actuator holders as shown in figure 10 individually, and the probe was positioned at 10 mm a distance away from the center of the essence of the electromagnetic coil.

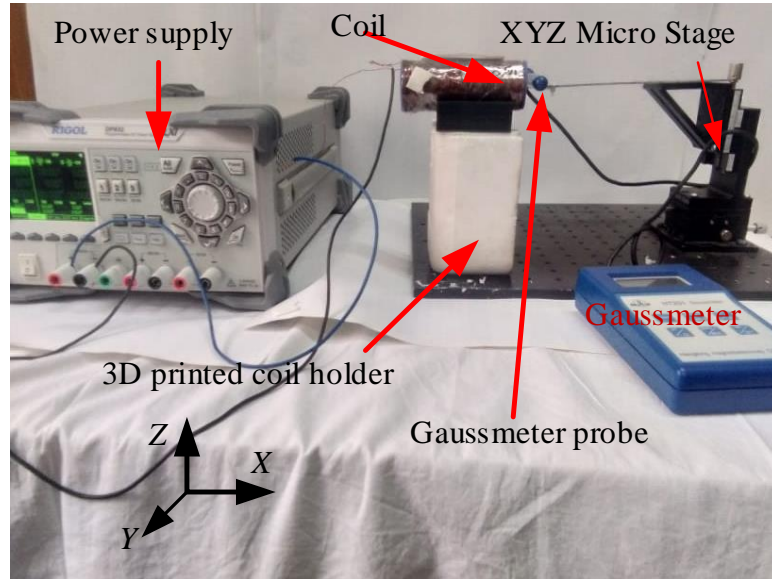


Figure 0.3 Experimental setup for the coils to test the coils parameter such as length, current, and distance from the central axis of coils.

3.3.2 Experimental Results

Electromagnetics coils shown dipole magnet on energizing by apply current which are shown in figure 3.4.

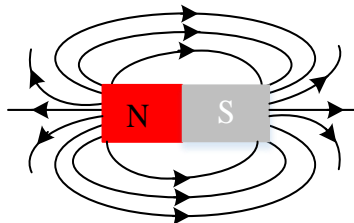


Figure 0.4 Electromagnetics coils shown dipole magnet on energizing by apply current.

The first experimental is performed to test the length of an electromagnetic coil on magnetic field results are shown in figure 3.4 proves that actuator length has an inverse relation to the magnetic field which is nicely validated with a mathematical model is presented in equation (1.1). The graph in figure 3.4 successfully validates the relation of length on the magnetic field given in equation (1.1).

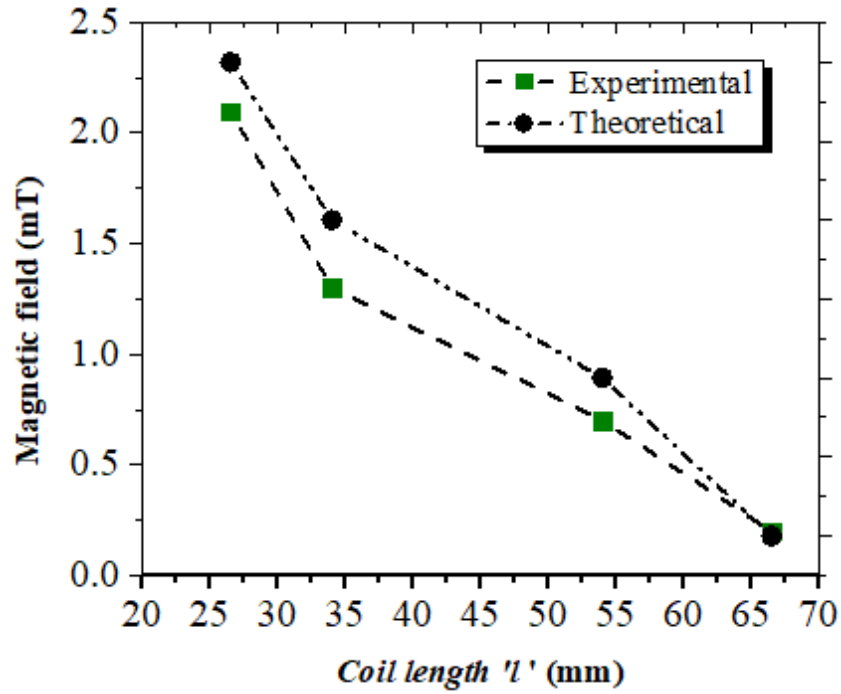


Figure 0.5 graph between the coil length 'l' (mm) of the coil and magnetic field(mT)

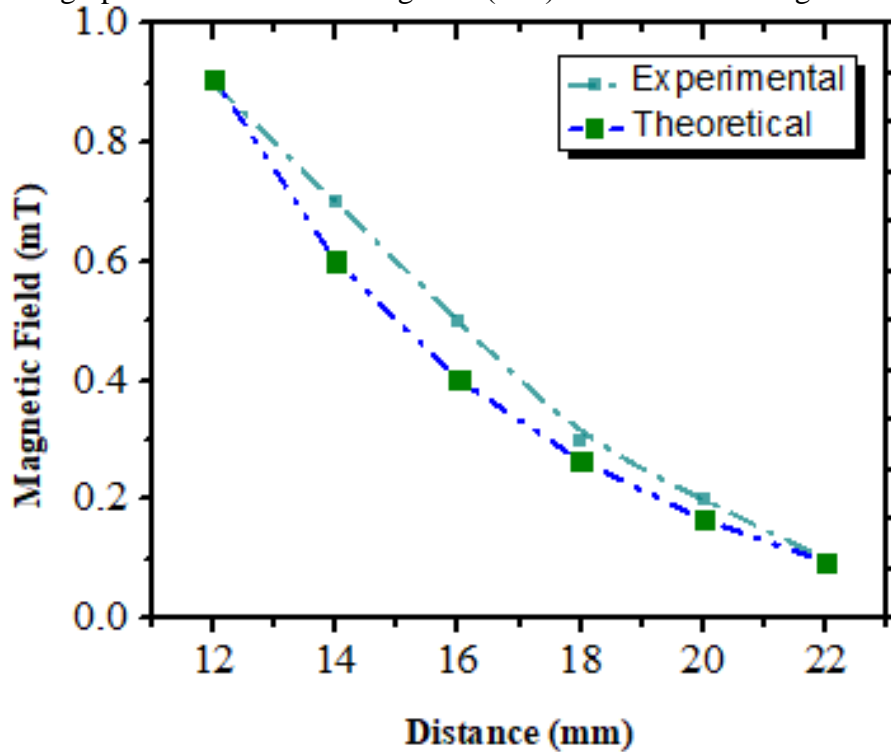


Figure 0.6 The graph between distance(mm) from the central axis of the coil and magnetic field (mT)

To assess the effects of 'r' on the magnetic field, the magnetic actuator of the length of 100 mm, 15855 number of turns while to excite the voltage 10 V and current were 0.15 A. By

utilizing the micro-stage on X-axis, the probe of the gaussmeter is mounted away from the central axis with a motion resolution of 2 mm. The result in figure 8, shows an inverse relationship between the magnetic field and 'r' which is showing a good agreement with equation 2. The probe was moving along the X-axis and Z-axis to measure the field variation along an imaginary plane at the probe distance of 10 mm from the electromagnetic coil. As shown in figure 3.6 the magnetic field reduction while moving out from right in the middle of the coil.

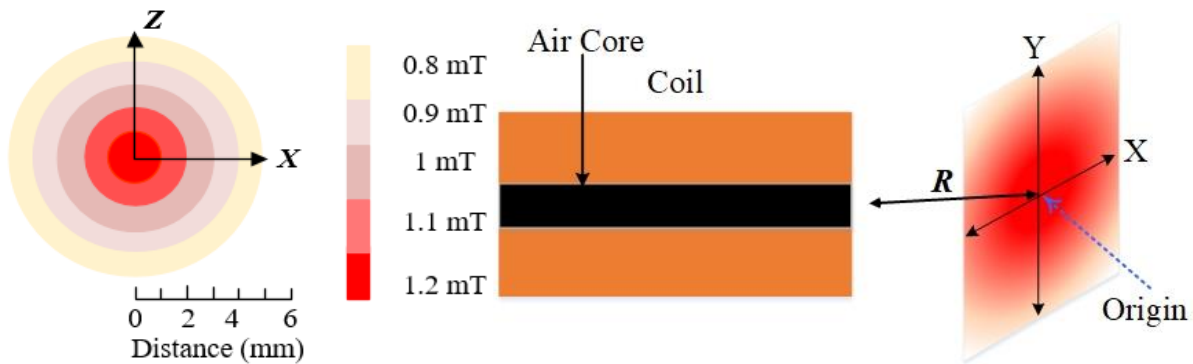


Figure 0.7 (a) Measured 'B' along X-axis and Y-axis on a plane at distance 'R' = 10 mm from the coil, Centre of the longitudinal axis Centre of the core is taken as the origin (b) Measurement scheme of magnetic field on a plane at distance 'R' from the Centre of the core.

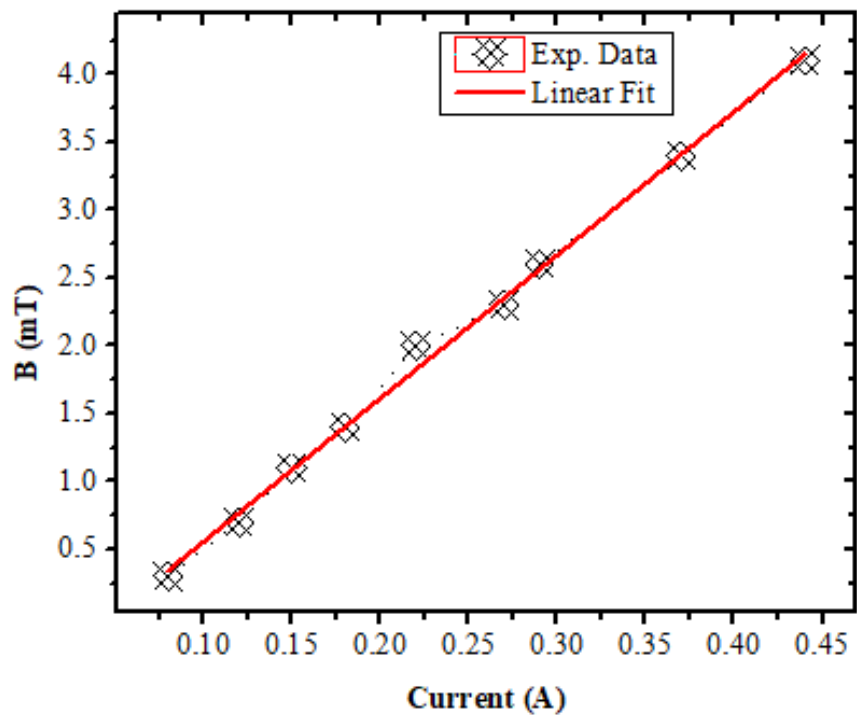


Figure 0.8 The graph between the applied current and the magnetic field

In figure 3.12 demonstrated the measurement schematic of coil measurement. This experiment evaluates the relationship between current and magnetic field. In this experiment, different currents were applied to the same coil ($N=15855$, $L=100$ mm, $I=0.55$ A) graph against values in figure 3.10. Current is directly proportional to the magnetic field strength as demonstrated in figure 3.10 and experimental findings are in excellent agreement.

Conclusion

The chapter demonstrates the design of coils and how their parameters affect coil magnetism. The number of turns is directly proportional to the magnetic field. As the current increase, the magnetic field also increases. Distance is inverse to the magnetic field, and it means as distance increase the magnetic field decrease. In this chapter, we successfully verify the Biot-savant law.

CHAPTER 4. DESIGN AND DEVELOPMENT OF 2-DOF MAGNETIC MANIPULATION SYSTEM

In the last few decades, magnetic systems are widely used. Wirelessly controllable microrobots have lots of applications in biomedical and other fields of science. These microrobots change the traditional ways of treatment. Due to the micro size of robots, it is difficult to powering and actuation/control. In this way, magnetic actuation shows very good performance as well as ease to control with a better response. Which makes it perfect for industrial in the same way as for the in-vivo and in-vitro application.

Several researchers and their teams work on magnetic actuation and make tremendous progress. Electromagnetic system based on three types of coils systems Helmholtz, Maxwell, and cylindrical coils system. Helmholtz is shown in figure 4.1 (a) based on identical electromagnetic coils and the gap between them is equivalent to the radius of the coil. Each coil contains current carried equal and same direction, and it produces a homogeneous magnetic field as shown in figure 4.1 (b) which is used for the rotation of magnetic microrobot. On the other hand, maxwell as shown in figure 4.1(c) also has identical coils with the radius equal and the equal number of turns but their distance between them is equal to three times their radius and current is the same but opposite in direction. It can generate a uniform magnetic gradient as shown in figure 6(d).

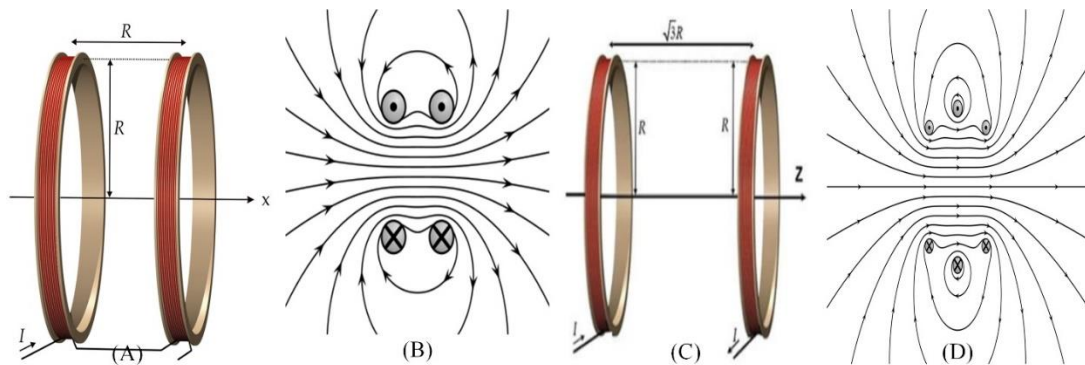


Figure 0.1(A) and (B)The Helmholtz,(C) and (D) Maxwell, and their generated field [4].

For the linear and rotational Helmholtz and maxwell were both used in combination, However, this kind of system has been agony from a geometric vulnerability i.e., the length of unit-pair must be twice to the other. Hence, this kind of system requires a large space and a considerable amount of electric power to generate an effective and efficient magnetic field.

4.1 Design and development of Magnetic system

In step, we developed two pairs of cylindrical coils-based prototypes as shown in figure 4.2 (a). then we design the coil holder in solid work as shown in figure 4.2 (b) in the last step we develop a prototype which is shown in figure 4.2 (c). Single pair of coils is used to move the microrobot move alongside the x-axis and the y-axis.

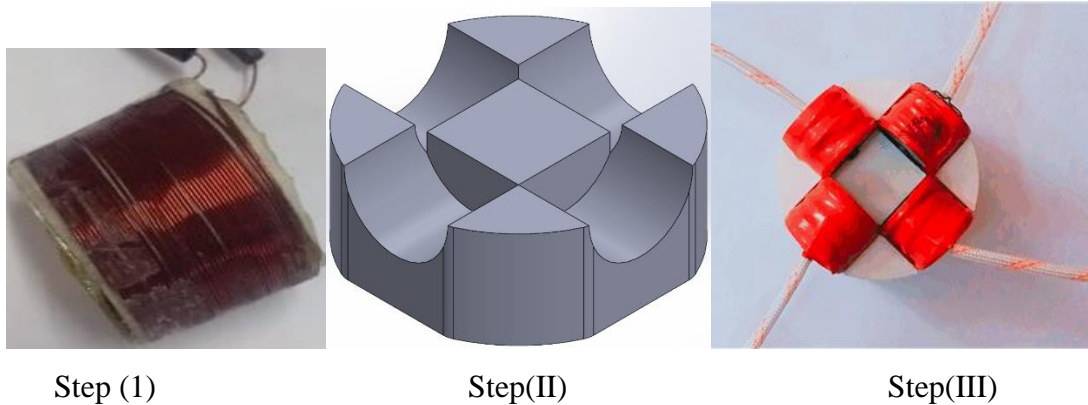
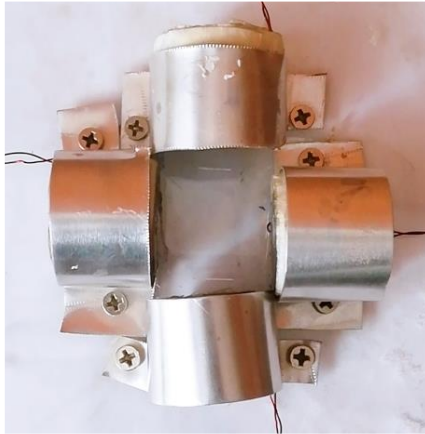


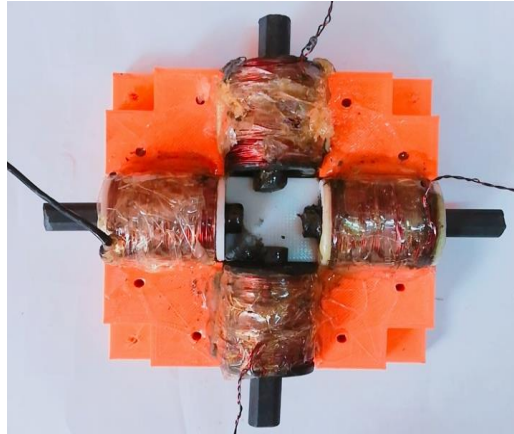
Figure 0.2 Step(I) developed electromagnetic coil. Step(II) CAD design of assembly holder step (III) developed coils are mounted on the 3D printed coil holder.

First step we design the spinal and holder in solid work and then did a 3D print by using a 3D printer (Crealty CR-10-S5). In this research, three different prototypes are designed using cylindrical coils. The first one is an aluminum-based system with the base plate made of glass as shown in figure 4.3. This setup has two geometrical problems such as misalignment and magnetic field interference. Firstly, misalignment occurs along the Y-axis as shown in figure 4.3(prototype I).

However, no effect on the magnetic field along Y-axis is observed. Secondly, magnetic field interference occurred due to the inclusion of iron screws used to hold the aluminum strips. The second prototype as shown in figure 4.3 (prototype II) is made of 3D printed. All parts including the base plate and bobbin are fabricated using 3D printing. A winding machine is used to count the number of turns and resistance as shown in table 4.1. Magnetic field results along the $\pm X$ -axis and $\pm Y$ -axis are shown in Table 4.1. The third prototype is made of aluminum and 3D printed as shown in figure 4.3 (prototype IV). A bobbin is made of aluminum and the actuator is 3D printed. The number of turns, coil length, resistance, and the magnetic field are mentioned in table 4.1.



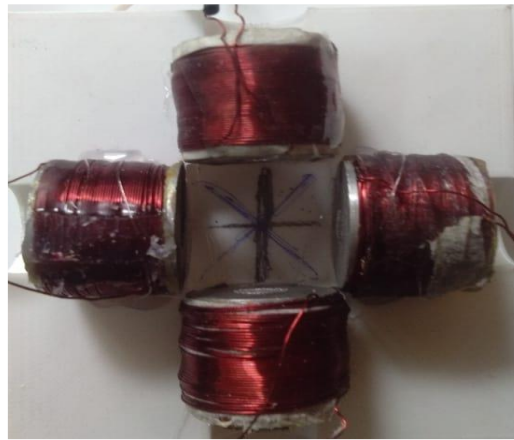
Prototype I



Prototype II



Prototype III



Prototype IV

Figure 0.3

Our earliest developed prototype (I) consists of aluminum and hold on the acrylic sheet. Prototype (II) based on the 3D printed part. Prototype (III) the bobbin is made of aluminum and holder is 3D printed. Prototype (IV) is same as prototype (I) we developed to remove the miss alignment of prototype (I).

Table 0.1 Specifications of developed prototypes.

Prototypes	Number of turns for each coil (N)	Resistance of each coil (Ω)	Coil length (mm)	The magnetic field at the Centre of ROI	Core
I	600	6.5	24.50	4.4	Air ($l=24.5$, $D= 8.5$ mm)
II	910	7.1	35.50	26	Ferrite ($l=60.5$, $D= 10.5$ mm)
III	210	1.5	15.50	3.65	Ferrite ($l=16.5$, $D= 3.5$ mm)

4.1.1 Impact of core

The magnetic core is a piece that is used to confine and guide magnetic fields in electromagnetic systems made of magnetic material with high magnetic permeability. Its material is based on ferromagnetic materials such as ferrites or iron. It is used to concentrate the magnetic field lines in the core material because it has more high permeability relative to the air in its surroundings.

A magnetic field is created by applying current on the coil wire wound around the core. We used a ferrite core rod. In figure 4.1 (a) comparison of the ferromagnetic (μ_f), paramagnets (μ_p), diamagnets (μ_d), and free space (μ_0). An external magnetic field is created by applying current "I" its magnetic field in ferrite by aligning tiny internal dipole in the material.

Moreover, the current and external fields are reached zero. the core remains partially magnetized the curve is shown in figure 4.4 (b)

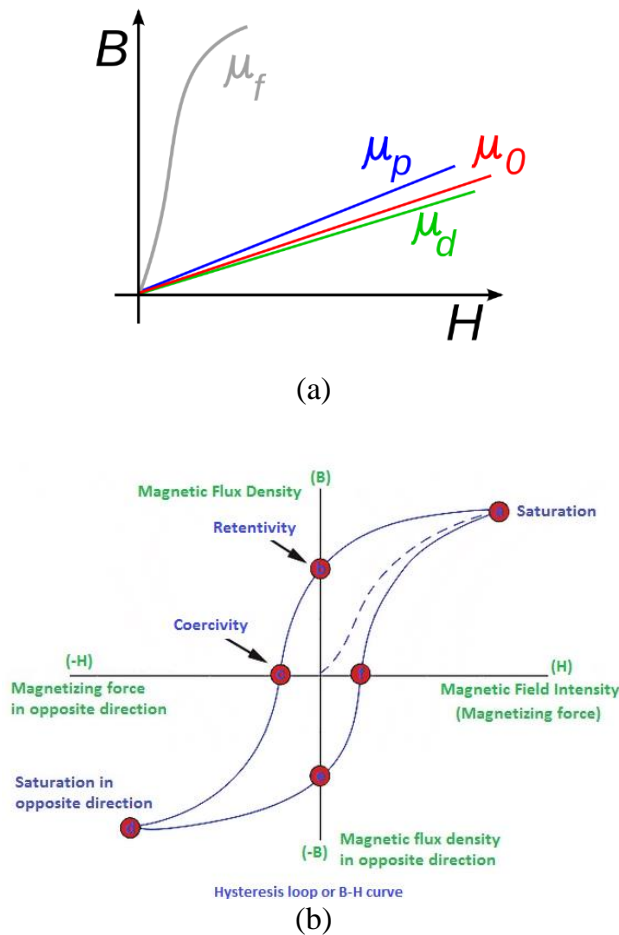


Figure 0.4 (a) A comparison of different permeability (b) hysteresis loop and for the magnet cycle [72].

4.2 Magnetic Field characterization of the developed systems

4.2.1 Magnetic Field Characterization System

To attain high-resolution micromanipulation of a magnetic robotic, it's miles essential to symbolize the system to generate a correct version to map system inputs to robot behavior. This section discusses the characterization of a magnetic actuation system that consists of tetrad the same electromagnetic coils that will be used to manipulate a magnetic micro-robotic as shown in figure 4.5. We introduce an empirical characterization technique to parameterize the device.

Reliable manipulation is important to have a spatial illustration of the magnetic subject to avoid growing areas of high variability within the magnetic discipline gradient close to the robotic. Furthermore, the manage algorithms proposed hinge on exploiting the spatially nonlinear magnetic area gradient to independently manipulate multiple robots. Accordingly, to reap sub-millimeter precision in robot position, it's far critical to have a correct version that maps the vector of entering currents into the actuator to the spatial magnetic area during the workspace. Developing a correct version of the magnetic discipline is challenging because most magnetic manipulation systems, along with our own, are custom constructed. Variability can get up in custom-built structures if the electromagnetic coils are hand-wound.

Additionally, rapid prototyping techniques and one-off designs can cause low tolerances on measurements. For these systems, there does now not exist a fixed of specifications that element the form of the magnetic area generated via each electromagnetic coil and the electricity of the sphere. Even as electromagnetism is well studied and there are analytical equations that govern the magnetic field created through the modern-day through a wire, implementing these equations usually entails making a few assumptions. Furthermore, a number of these equations do now not keep for our gadget because the workspace is close to the workspace. To validate a version, we want to measure the magnetic discipline. There is a massive range of commercially to be had tools for measuring magnetic fields. We needed to select one with two axes of dimension and a small shape factor that allowed it to be maneuvered around the workspace.

We function near the electromagnetic coils because the magnitude of the magnetic subject decays at a rate of distance to the third electricity. As a result, using a factor dipole version based on the geometry of the coils does now not generate a correct version of the magnetic subject. In this version, we count on that the magnetic fields linearly superimpose and that neighboring electromagnetic coils do now not interfere with one another. Furthermore, we attempt to shape

the magnetic discipline measurements to a degree-dipole model parameterized to healthy empirically measured information.

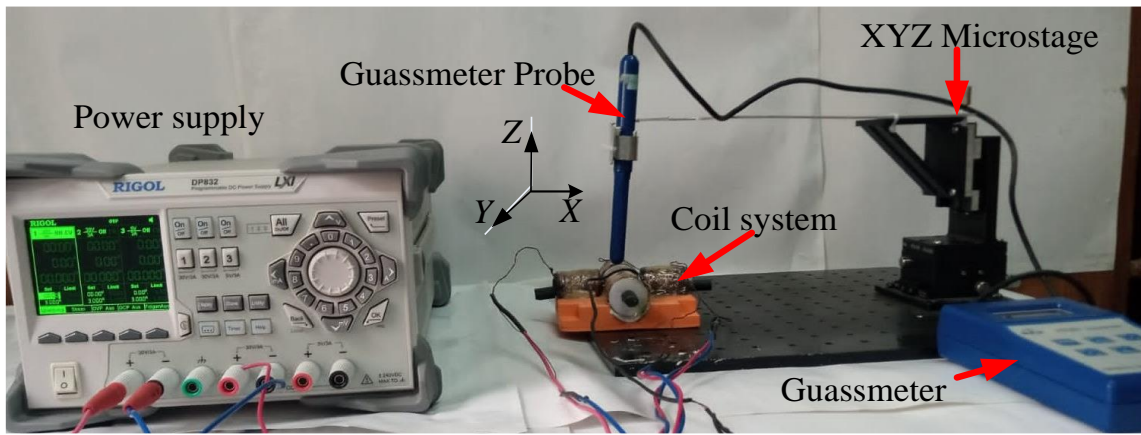


Figure 0.5 Experimental setup to observe the field effects in the workspace in this setup Gaussmeter meter probe is mounted on the XYZ stage.

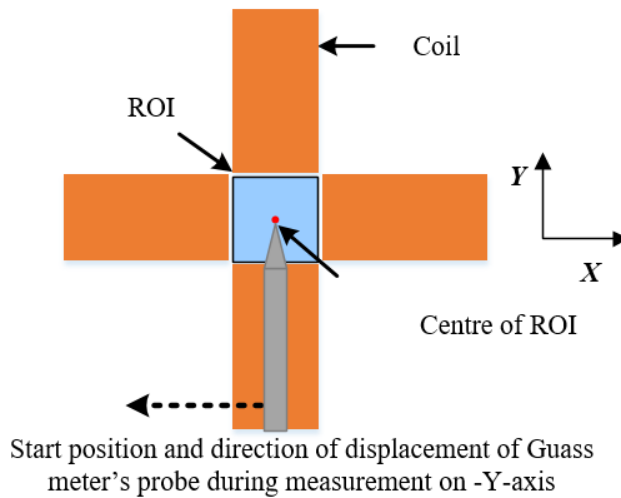


Figure 0.6 Measurement scheme in which schematic of coils, ROI center, and ferrite core base rod for measuring the magnetic field of the developed systems.

First, a magnetometer, HT201 is used to measure the magnetic area experimental setup is shown in figure 4.5 which is discussed in the early section in chapter 3. We kept the Gauss meter probe at the Centre of the workspace and excite the coils to measure the values of the magnetic field. It is crucial to fix the probe to avoid the vibrations of the magnetometer which is necessary to decrease errors. Figure 4.6 demonstrates a measurement scheme in which schematic of coils, ROI center, and ferrite core base rod for measuring the magnetic field of the developed systems.

4.2.2 Single Coil Excitation and Magnetic Field measurement

In this experiment, we measure the magnetic field by energizing coils one by one for all prototypes by using an experimental setup for which is discussed earlier in sections. Applied current was 1.5A and the voltage limit was 12V by using power (EGOL DP 830 programmable power supply) and take all measurements by Gauss mater (HT201) and in figure 4.7 the values are about X, (-)X, Y, and (-) Y-axis are shown. And figure 4.8 shown values represents the values around XY- axis.

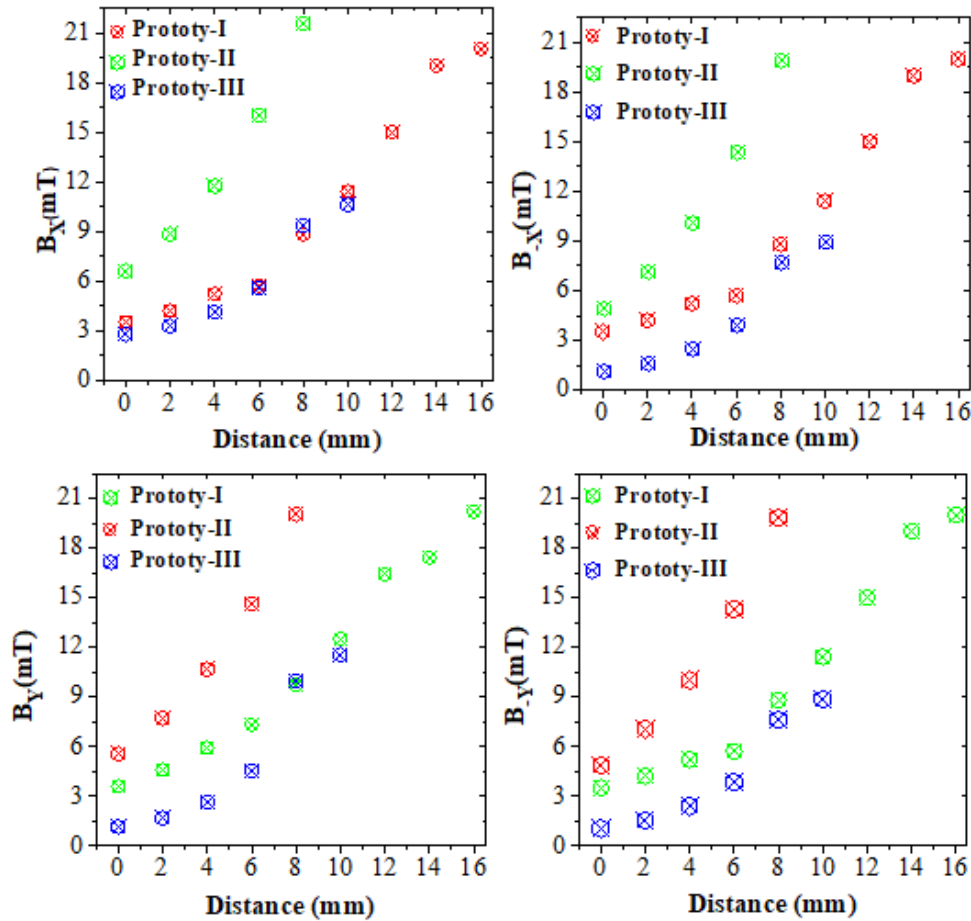


Figure 0.7 Measurement of the magnetic field along $\pm X$ - and $\pm Y$ -axis when moving tip of tesla meter from the center of ROI toward the coil with a motion resolution of 2 mm where its current value was set as 1.5 A.

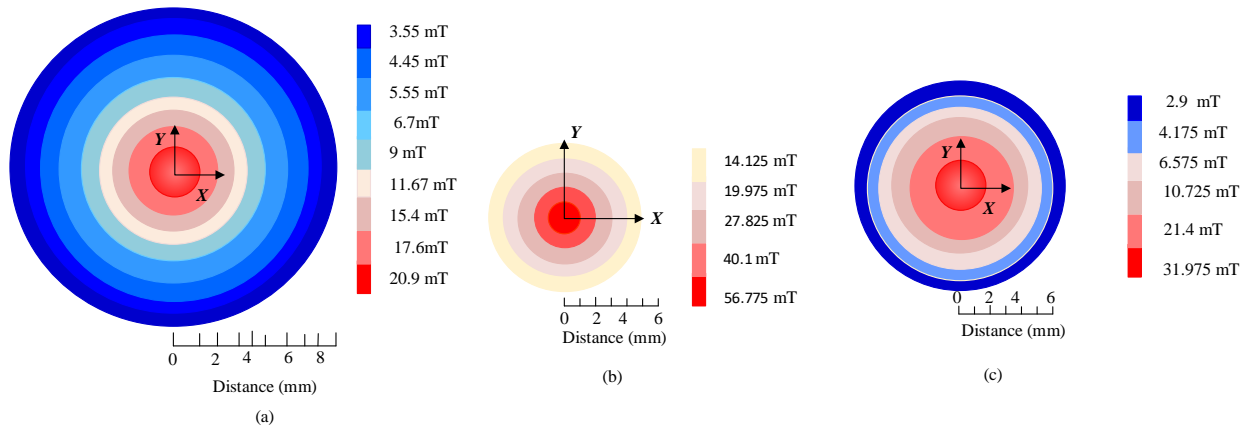


Figure 0.8 Visual representation of the measured data on XY -plane.

4.2.3 Simultaneous Excitation of four coils and Magnetic Field Characterization

Electromagnet coils act as a magnet on the applying of current. The force between It has also shown the north and south poles. For the indication of the pole, we use a bar magnet with indicated north and south poles. The same poles have repulsive forces and different attracted each other. For the experiment, we apply a current of 0.5A and the by using firstly to indicates the north and south pole use bar magnet and then by using of gaussmeter measure the magnet field values.

4.2.3.1 Quadrupole Configuration

All magnetic sources always have a dipole field. it is very easy to make a magnetic quadrupole by putting coils in the same coil in a quadrant manner. There are four tips we have in the workspace by managing them we can arrange them in three manners and observe their magnetic field and force. As shown in figure 4.9. In figure 4.9 (a) is the first configuration (I) in which $-X$ and $-Y$ -axis coil are the south poles inside and X and Y north inside the become between the Y and $-X$ -axis coil and the X and $-X$ axis coil. First, we turn on one by one coil and measure the magnetic field which is given in table 4.2. Configuration (II) when X and Y -axis coil are south inside and other two $-X$ and $-Y$ -axis coils are north inside this configuration magnetic field at the center of the ROI is zero but the at all corners have a magnetic field as values are given in table 4.2. In configuration (III) is shown in figure 4.9. In which all coils are north inside and south outside. In this configuration, each coil repels the other because all have the same pole. At the corner of the workspace magnetic field is equal to zero. Then we measure

the values in front of coils, and they also lose their magnetic field. Magnetic field values are shown in table 4.2.

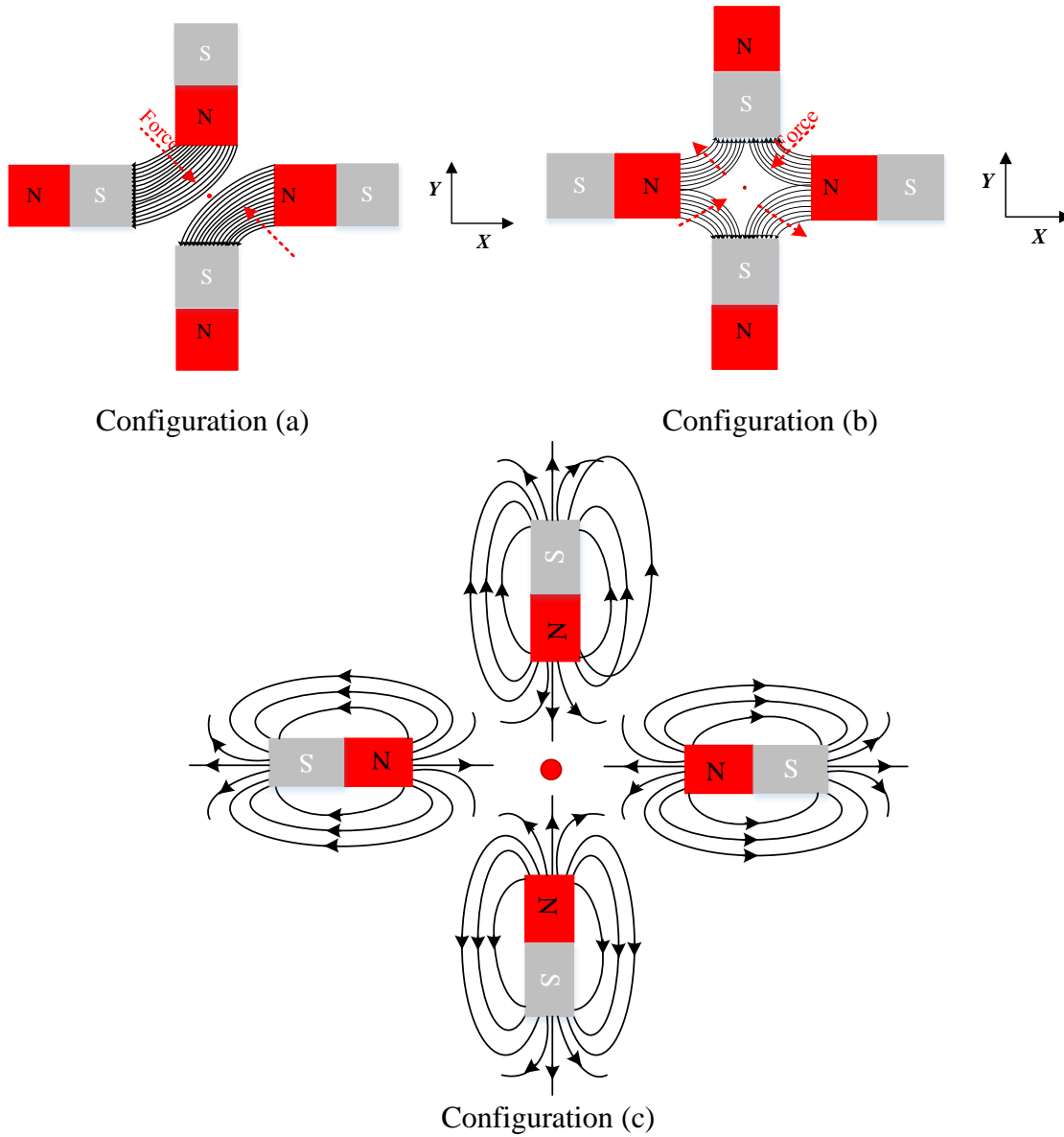


Figure 0.9 (a) Quadrant pole configuration when $-X$ and $-Y$ are internally south and X and Y are North from internally. (b) when X and Y are south internally and $-X$ and $-Y$ are North. (c) when all are north inside.

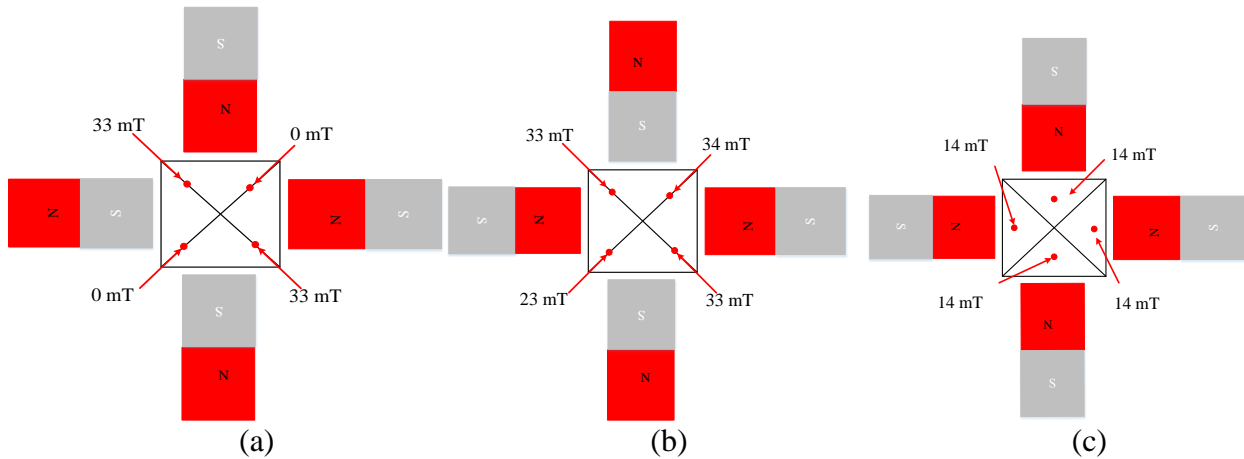


Figure 0.10 (a) Measured values for configuration (a). (b)

Measured values for configuration (b). (c) Measured values for configuration (c)

Table 0.2 Magnetic field by energizing one by one and then energizing.

Configuration	Magnetic field Values on energizing one by one (mT)		Magnetic field values after all energized (mT) at corner	
	Axis	Value	Corner	Value
Configuration (a)	<i>X axis</i>	40	Corner between <i>X and Y axis</i>	0
	<i>- X-axis</i>	43	Corner between <i>X and -Y axis</i>	25.4
	<i>Y axis</i>	41.5	Corner between <i>-X and -Y axis</i>	0
	<i>-Y-axis</i>	48	The corner between <i>-X and Y-axis</i>	26
Configuration (b)	<i>X axis</i>	43	Corner between <i>X and Y axis</i>	34
	<i>- X-axis</i>	41.7	Corner between <i>X and -Y axis</i>	33
	<i>Y-axis</i>	43	Corner between <i>-X and -Y axis</i>	23
	<i>-Y-axis</i>	48	The corner between <i>-X and Y-axis</i>	33
Configuration (c)	<i>X- axis</i>	35	14	
	<i>- X-axis</i>	35	14	
	<i>Y-axis</i>	35	14	
	<i>-Y-axis</i>	35	14	

4.2.3.2 Same poles facing inwards

In this experiment same poles facing inwards. Which have strong repulsion to word each other. The magnetic field has zero at the center of the ROI. Near the coils, it also reduces the magnetic field.

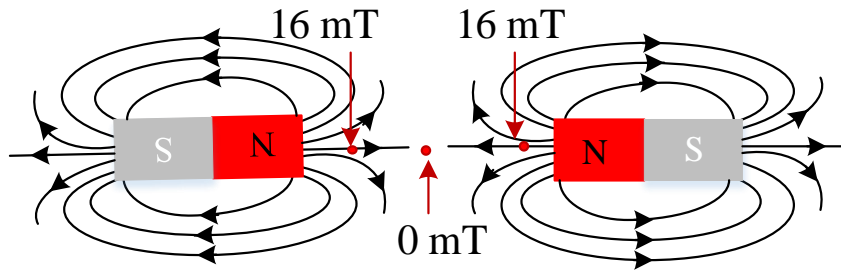


Figure 0.11 Same poles facing inwards

4.2.3.3 Collinear Coils facing opposite poles

On the current, the magnetic coils act like a magnet. In magnetic one pole act like south and the other act like a north pole and same pole repels each other. But opposite poles attract each other. The value of magnet field is 25.6 mT, at (-) X-axis is 41.5mT and 41mT magnetic field.

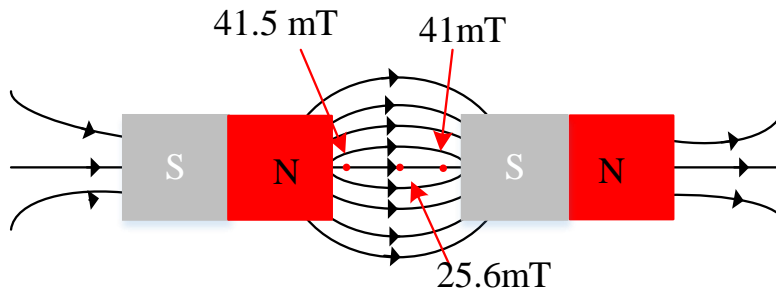


Figure 0.12 Collinear Coils facing opposite poles

4.3 Micro Robotic Manipulation System

Micro robotics setup consists of the computer, controller system, Actuator, workspace, and feedback as shown in figure 4.13.

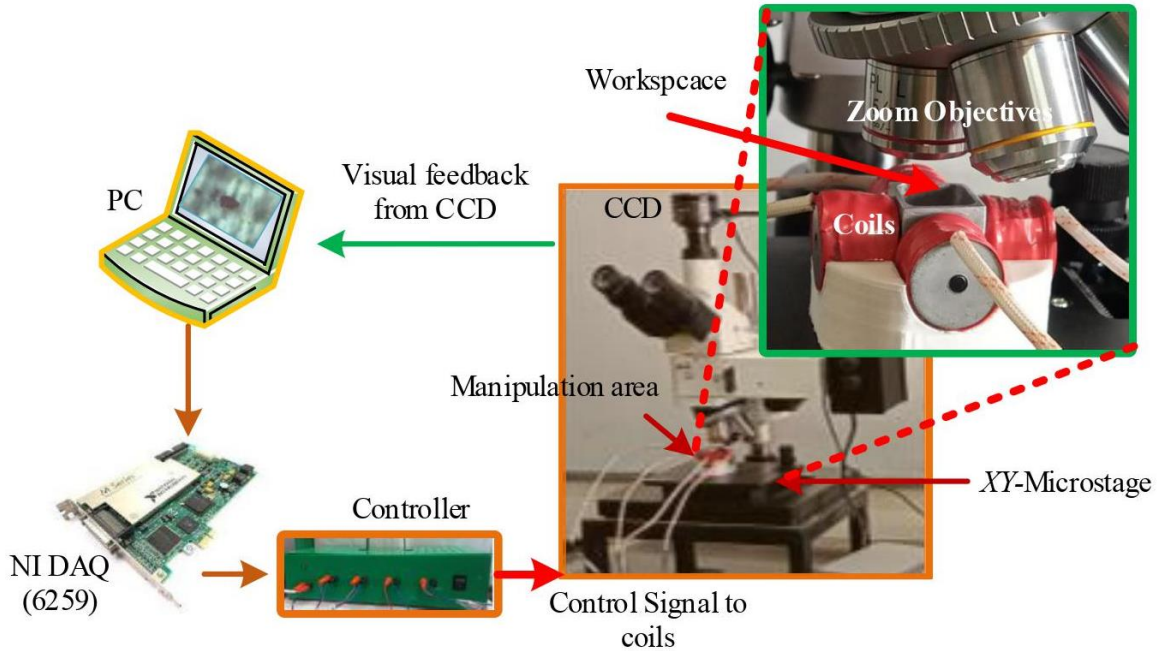


Figure 0.13 Schematic diagram of the system which consists of DAQ(6259), XY stage for the motion of workspace, pc, and 2D coil system.

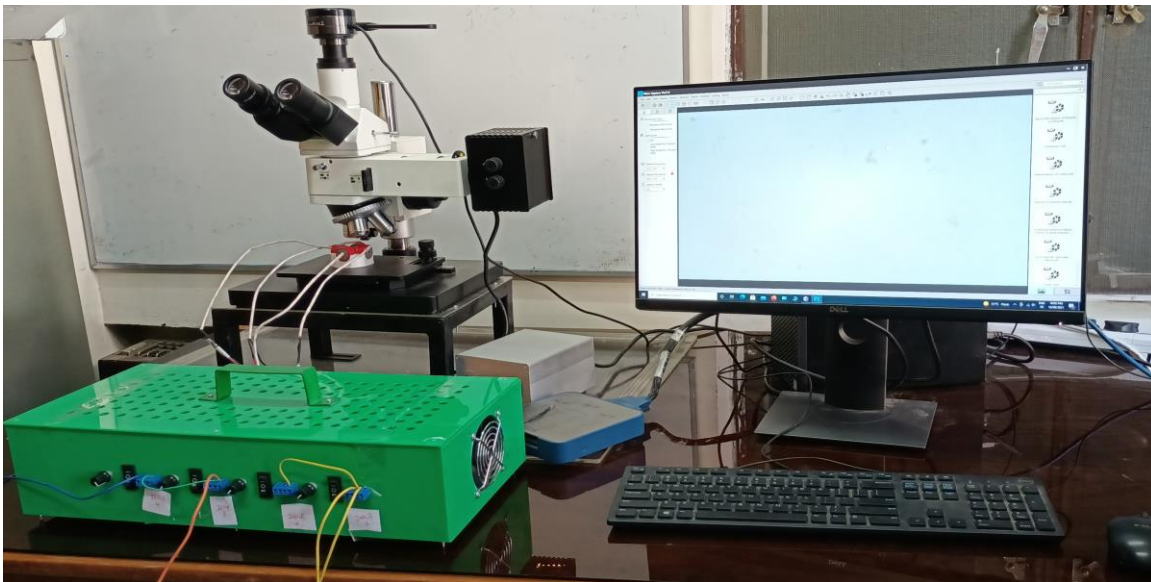


Figure 0.14 Complete magnetic micro-robotics System for the 2D motion of microrobot.

Figure 4.14 shows the complete magnetic microrobot system which consists mainly of two-axis electromagnetic coils that can generate static and dynamic magnetic fields, Olympus microscope equipped with lenses of 5 \times , 10 \times , 20 \times and 50 \times that enable high-resolution visual feedback, an NI DAQ (NI-PCI-6359) to generate a control signal and four motor drivers (MD25HV) to excite each coil which can provide output current 25A, more details about the

setup are given in table 4.1. our prototype (b) which is discussed in early sections can be 26mT at the current of 1.5A. which is continued and effective to diver microrobot without temperature variation. A national instrument DAQ card (NI-PCI-6359) was used to provide the controlled signals. The control algorithm is developed by using a Software visual studio for C programming. In control to achieve a wide range of locomotion of the microrobot, the micro-robotic setup is mounted on the X-Y stage with the range of 18 mm and resolution of $1\mu\text{m}$ on both axes. X-Y stage is used to adjust the image of the area in real-time which helps to simultaneously localization of microrobot. the complete system diagram is shown in figure (4.14). Electrical circuit diagram to control the 2D motion of the microrobot system is shown in figure 4.15.

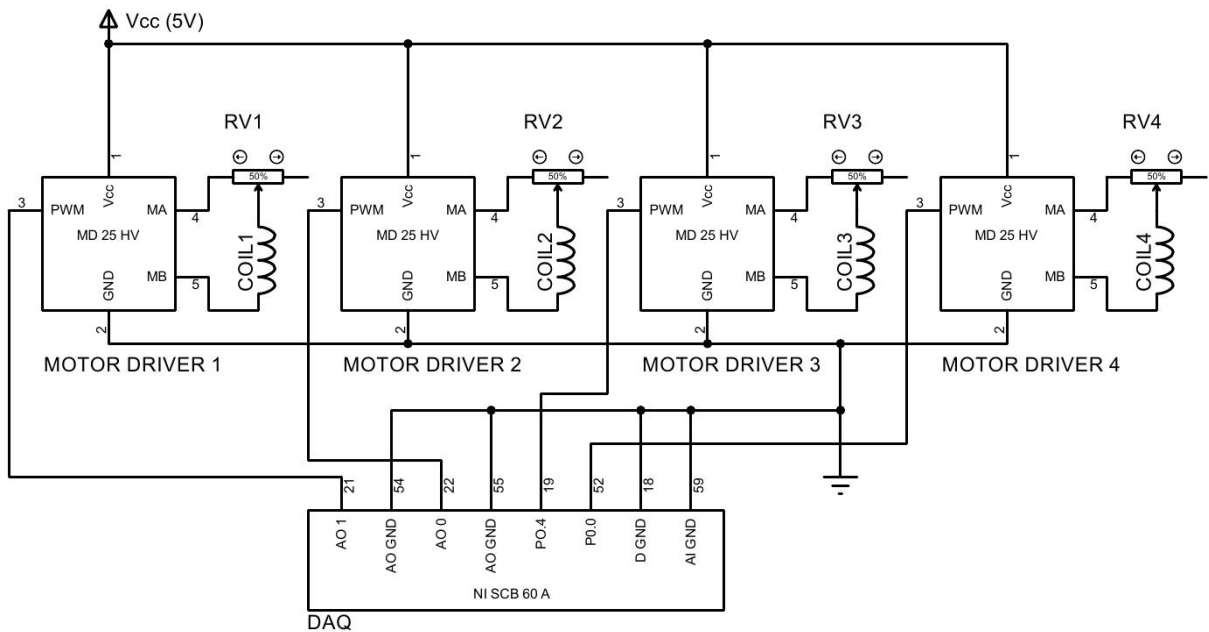


Figure 0.15 Electrical circuit diagram to control the 2D motion of the microrobot system.

4.4 Motion control of magnetic microrobots

This kind of actuation system depends upon the pulling force of microactuators for the actuation of the microrobot. To make microrobot's motion in any plan four identical in-plane electromagnetic coils can be energized in pair form or also individually. The robot used should have magnetic or magnetizable properties. The position of the microrobot realizes on the applied current on electromagnetic coils. It is a very effective transportation style used for the actuation

system. The spherical body of the microrobot is very efficient at tracking and very useful for stabilizing the microrobot when it is being pulled and pushed.

Ferro-magnetic-based microrobots are demagnetized after the experience of hysteresis, the is a procedure whereby the magnetization of the magnets will be either one gained or dropped over a large area. Saturation magnetization is called when the microrobot gains its top magnetization then M is the microrobot magnetization vector in the direction of magnetitic field B . Once the microrobot is energized by applying the external field and then the magnetic field is removed the microrobot will have microrobot remanent magnetized. Moreover, if the ferromagnetic microrobot's intrinsic coercivity is equal to the field H and the magnetic field is applied in the opposite direction of magnetization vector M then the microrobot will lose its magnetization. If the microrobot lost its magnetization or is demagnetized it will become inactive, ineffective, and unresponsive. By minimizing the angle of B and M then instead of demagnetization torque will be produced. As equation is given in Torque produced on a microrobot is given Eq. 4.1.

$$T_{m=M \times B} \quad (0.1)$$

Eq. (4.1) demonstrates the relationship that how the microrobot aligns to the B magnetics field. There are no flux lines and force when the microrobot is away from the line centerline. However, when the microrobot is at the center axis to the dipole moment field of source magnetic pull microrobot to the near the source.

$$F_m + F_d + F_b + F_g = m \frac{dv}{dt} \quad (0.2)$$

Here in equation "v" is the velocity of microrobot force analysis is given below section. Horizontal direction force acting on microrobot against the motion. In order to move the microrobot applied force must be greater than the resistance observed by the microrobot.

$$F \gggg F_d + F_b + F_g \quad (0.3)$$

Where F is the applied force on microrobot and F_d is the resistance applied by the environment of the microrobot

$$F_m = V(M \cdot \nabla)B \quad (0.4)$$

At the center of the axis or near to it the dipole moment is ∇ , the force F can be described as in Eq. (4.4), where B is the magnetic field, M magnetization of the microrobot and V is the volume of the magnetized object.

In this experimental setup, the coils of the electromagnets are bigger than the working space relatively. It can be lying at the center of the center axis of the electromagnetic coil. It

ought to be referred to that demagnetization is additionally restricted since the dipole of the microrobot is supported with the magnetic area, which limits the results of hysteresis.

$$\nabla = \begin{bmatrix} \frac{\partial}{\partial x} \\ \frac{\partial}{\partial y} \end{bmatrix} \quad (0.5)$$

$$M = \begin{bmatrix} M_x \\ M_y \end{bmatrix} \quad (0.6)$$

$$B = \begin{bmatrix} B_x \\ B_y \end{bmatrix} \quad (0.7)$$

Considering here only XY plane the magnetic force in vector form can be expressed as given below

$$F_m = \begin{bmatrix} F_x \\ F_y \end{bmatrix} = V \begin{bmatrix} \frac{\partial B_x}{\partial x} & \frac{\partial B_y}{\partial x} \\ \frac{\partial B_x}{\partial y} & \frac{\partial B_y}{\partial y} \end{bmatrix} \begin{bmatrix} M_x \\ M_y \end{bmatrix} \quad (0.8)$$

$$F_m = V \begin{bmatrix} M_x & \frac{\partial B_x}{\partial x} \\ M_y & \frac{\partial B_y}{\partial y} \end{bmatrix} \quad (0.9)$$

Here in equation (4.9) ∇B counter diagonal can be considered as Zero and M_x and M_y are constant magnetic field axis respectively. In such a way on the factor that can affect the force and direction are only $\frac{\partial B_x}{\partial x}$ and $\frac{\partial B_y}{\partial y}$. To produce magnetic field electromagnetic coils are required. The magnetic field can be generated by current flowing in coil wiring can be calculated by the equation given in early sections equation (3.1) and (3.2).

Three forces and weights are acting on the robot body. There are two forces and weight acting against the motion of the microrobot. For the movement of microrobot, the input force such as magnetic force should be overcome the surface tension and drag force. If weight and buoyancy force work in the opposite direction. Total forces acting on a robot are given in equation (4.10).

\vec{F}_m is the magnetic force applied by the external magnetic field, \vec{F}_d is the hydrodynamic drag force, $\vec{W} = F_g$ and \vec{F}_{buo} are weight and buoyancy force on the robot. As the robot is neutrally buoyant so only forces on the robot are \vec{F}_m and \vec{F}_d .

Weight and buoyancy force weight have three different conditions. First condition when

$$W < F_{buo}$$

In this condition when buoyance force is more than the weight of the robot, in this condition microrobot will be on the surface of the fluid. In this condition, the robot will be not stable, and it will move with the flow of fluid.

$$W > F_{buo}$$

In this condition, bouncy force is less than the weight of the microrobot. Lies on the surface of the workspace and a force is required for the uplift of the microrobot.

$$W = F_{buo}$$

In this condition will be in the middle of the fluid and weight and because bouncy force and weight are equal in these conditions robot will be stable and no need for the uplift force and it will F_m can work. If we consider our robot in this condition, then the weight and force of bouncy will be canceling each other. Then the equation (4.10) will become.

$$\vec{F}_{\mu Bot} = \vec{F}_m + \vec{F}_d \quad (0.10)$$

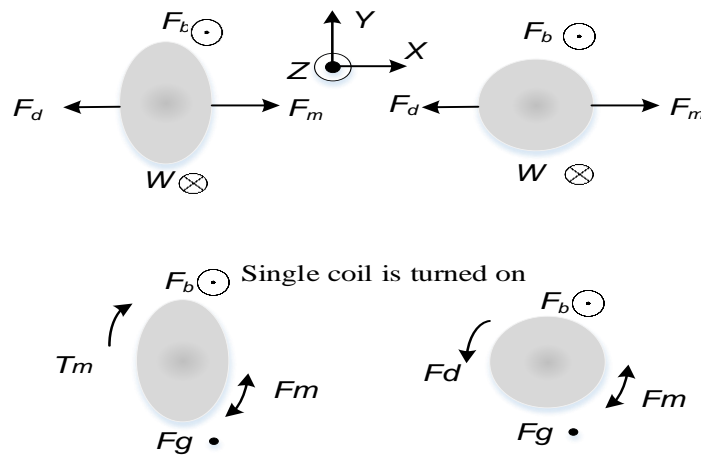
In equation \vec{F}_d is the hydrodynamic drag force F_m is a magnetic force as mentioned above.

$$F_d = \frac{1}{2} C_p A v^2 \quad (0.11)$$

Here in equation C is the drag coefficient, ρ fluid density, A is the area in front of fluid velocity v is the velocity in the direction of the normal plane. F_g is the gravitational force which plays a little role at low Reynolds number. At micro-objects engaged in liquid.

$$F_g = -V_p(P_p - P_f)g \quad (0.12)$$

In equation (4.12) V_p are the object volume, P_p is the object density, P_f is the fluid density, and g is the gravitational acceleration.



X and Y coils are alternatively turned on

Figure 0.16 Acting forces on the microrobot. F_m is a magnetic force, F_d drag force acting in a fluidic environment, and F_g is the gravitational force.

4.5 Magnetic Microrobots

Microrobots Fe_3O_4 is called magnetite naturally available as mineral main iron ore. It is ferrimagnetic and iron oxides. It has an attraction for the magnet and becomes itself a permanent magnet on magnetization. It is the largest magnetic of all other occurring minerals. On the discovery of magnetite (Fe_3O_4) the world of science was revolutionized with its attritive properties. It has tremendous applications such as electric motors transformers electromagnetic and biomedical applications.



Figure 0.17 (a) Magnetic powder for the magnetite (Fe_3O_4). (b) Iron particles collected after laser cutter machine we use these particles as microrobot in our experiment

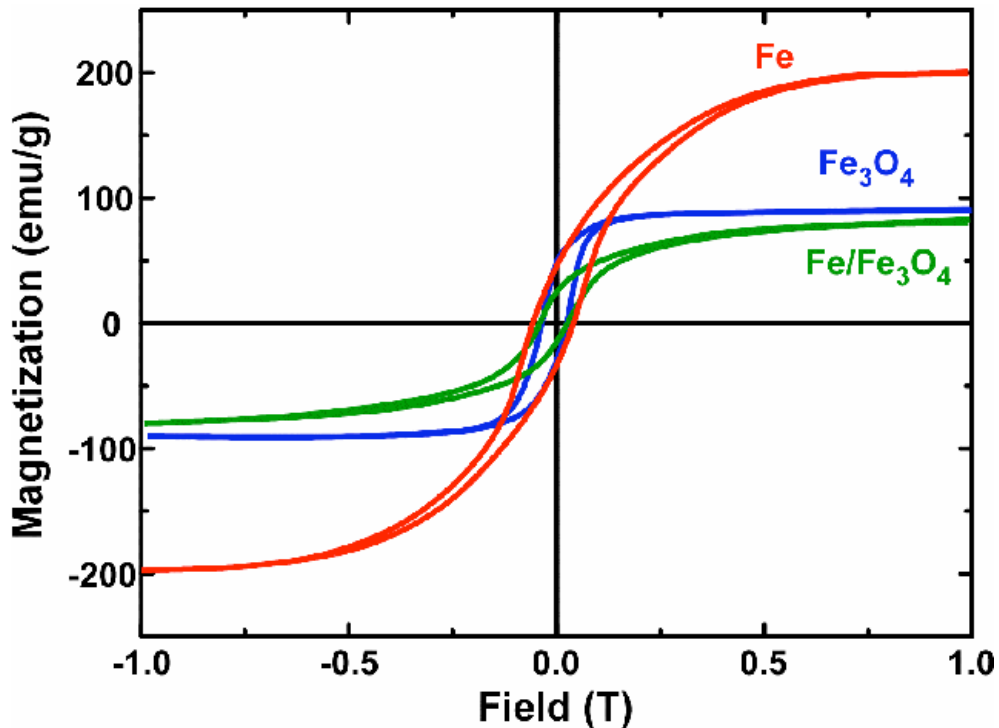


Figure 0.18 Hysteresis loop for the iron and the magnetite [73]

The major motivation for magnetite is the response of its particles under the effect of a magnetic field. when the magnetic field is applied to the sample of Fe and Fe_3O_4 it shows the state to bring the magnetization of saturation in figure (4.16) demonstrate the hysteresis loop for Fe and Fe_3O_4

Conclusion

In this chapter, we measure the magnetic field in the workspace by using a custom design system for the measurements of the magnetic field. Then different coils configurations measure the values of the magnetic field and observe how configuration affects the magnetic field values and such as when all same pole inside the workspace. we discussed a complete system for the manipulation and describe all components of a 2D micro-robotics system. Here for these experiments, we are using magnetite (Fe_3O_4) and iron particles as microrobots.

CHAPTER 5. EXPERIMENTAL RESULTS AND DISCUSSIONS

This section explores the usage of electromagnetic coils to control magnetic microrobots. We are proposing the force self-control technique to manipulate microrobots by using the space varying gradients of the magnetic field with static electromagnetic coils. We use a 2D planar system with four electromagnetic coils planned in a rectangle around as shown in figure 8 and discussed in earlier chapters.

5.1 Experimental Results

Four electromagnetic coils will be used to manage the movement of the magnetic microrobot alongside the x-axis and y-axis. Dual electromagnets are provided with the DC as an input to fluctuate the magnetic microrobot on the x-axis. The other two electromagnets controlling the movement of the magnetic microrobot alongside the y-axis. We can measure the location-tracking errors in the magnetic microrobot and the reference location using:

$$e_x = x_{ref} - x \text{ and } e_y = y_{ref} - y \quad (5.1)$$

Here e_x and e_y are the placement to monitor the errors all alongside the x-axis and y-axis, individually. Additional, X_{ref} and Y_{ref} are the ingredients of a reference to the location, and x, y is the placement of the magnetic microrobot. Orientation for the perspective of the microrobot θ is presented by equation 5.2.

$$\theta = \tan^{-1} \left[\frac{(|e_x|)}{(|e_y|)} \right] \quad (5.2)$$

Every electromagnet coil either generates the alternating domain or the uniform field. Our proposal for a control approach has been based on adjusting the magnetic microrobot, then swinging the magnetic fields to enable them for their swim or slide to a reference where the magnetic field is applied.

5.1.1 Rotational Motion

A Uniform magnetic field is used for the rotation motion of the microrobot. In figure 5.1, uniform magnetic fields are being applied by utilizing electromagnets coils Y and X-axis. And trembling motion of the Micro robotic Ice brags around 90 deg using a variable DC magnetic field is shown in figure 5.1 (I and II).

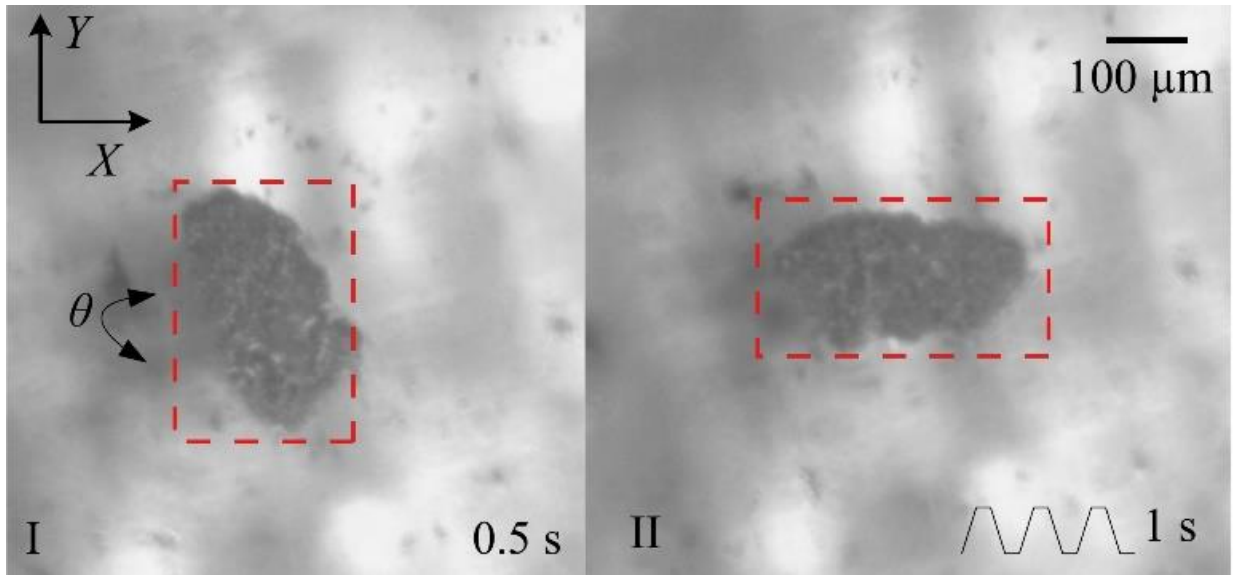


Figure 0.1 Trembling motion of Micro robotic Iceberg around 90 deg using variable DC magnetic field.

5.1.2 Linear motion

Open-loop movement control of the magnetic microrobot is accomplished by utilizing two opposing electromagnets coils to produce a magnetic field (right in the middle of the working space of the magnetic actuation system). By using the electromagnetic coils of the opposite electromagnet to swing these fields. Figure 5.2 represents an open-loop control movement outcome of the magnetic microrobots motion on the x-axis.

Now when $t = 0$ seconds, no electromagnetic fields are being applied by the electromagnetic coils, as well as the magnetic microrobot has no geared towards any axis as shown in Figure 5.1(I). then we energize the (-) x-axis coil when $t=32s$ it covers $100\mu m$ as shown in Figure 5.1 (II) the time $t=82s$ it covers $300 \mu m$ more as shown in Figure.5.1 (III) and when $t=122$ it covers $345 \mu m$ as shown in Figure 5.1 (IV) it covers $745 \mu m$ total distance and we notice that the magnetic microrobot moves at a speed of $6.1 \mu m/s$ by applying a current of $1.5A$.

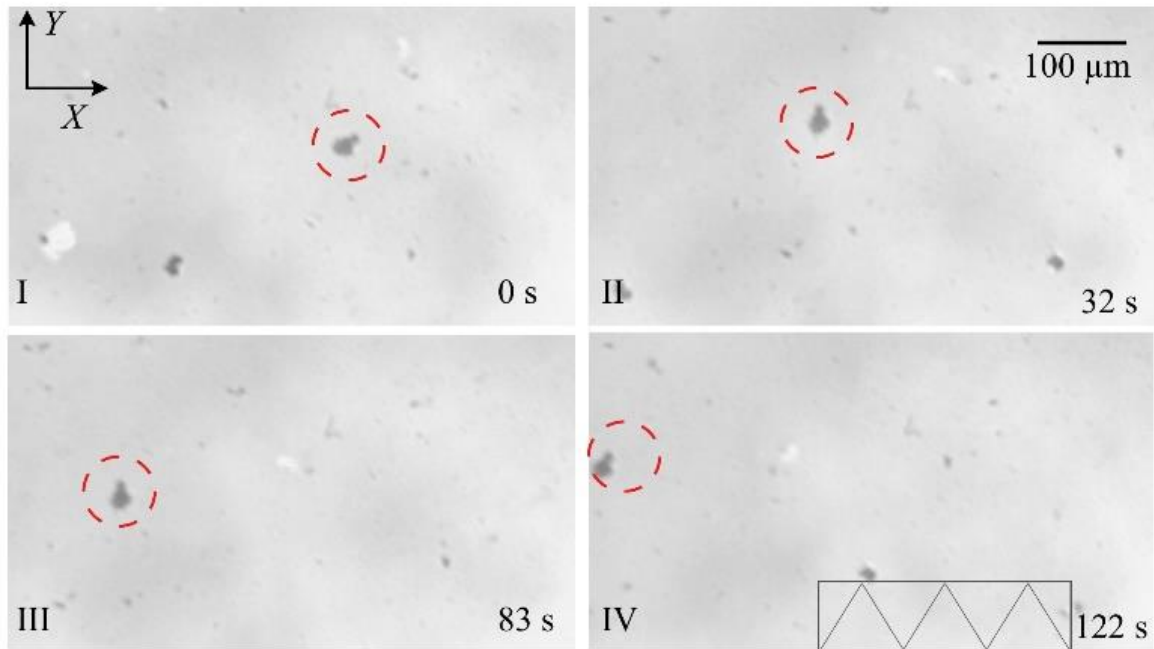


Figure 0.2: X-axis manipulation by using (-) x-axis coil.

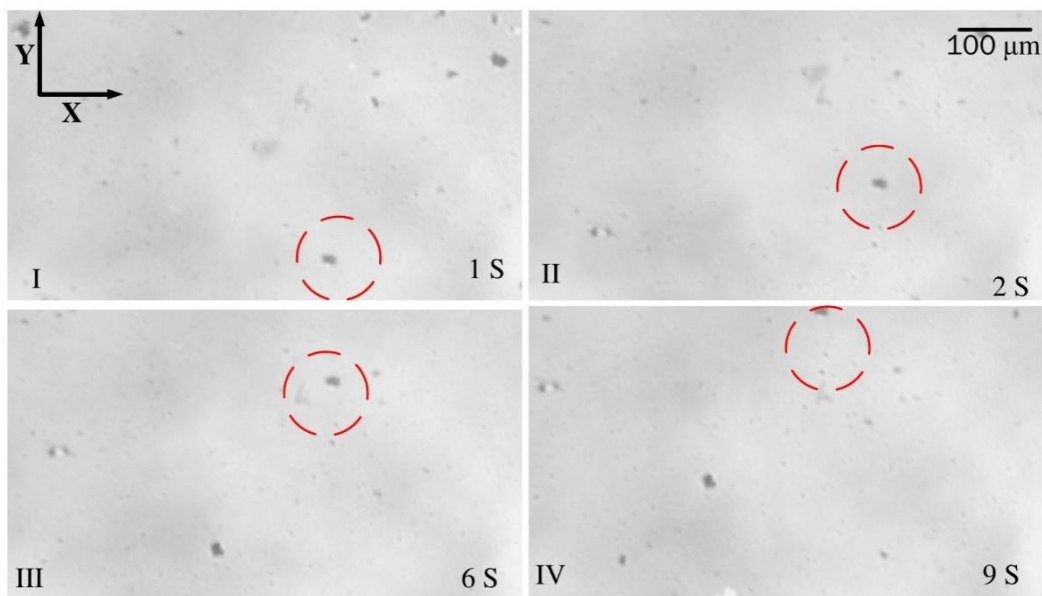


Figure 0.3 Microrobot motion around the *Y-axis* by using the *Y-axis* coils.

In the experiment, the magnetic microrobot comes into contact with the bottom by ionized water of the workspace of 18mm×18mm. The electromagnets coils of x and (-) x-axis did not energize so these coils have no magnetic field, although electromagnets coils of y and (-) y-axis generate uniform magnetic fields towards the reference position as shown in Figure 5.3 (I) when $t=0s$ and magnetic field have no excitement. In fig. 5.3 (II) when $t=1s$ it covers 10 μm . In

fig 5.3 (VI) microrobot's total distance is 350 μm . The Magnetic microrobot moves in the direction of the reference location and is located inside its surrounding area at the same speed of 12 $\mu\text{m/s}$.

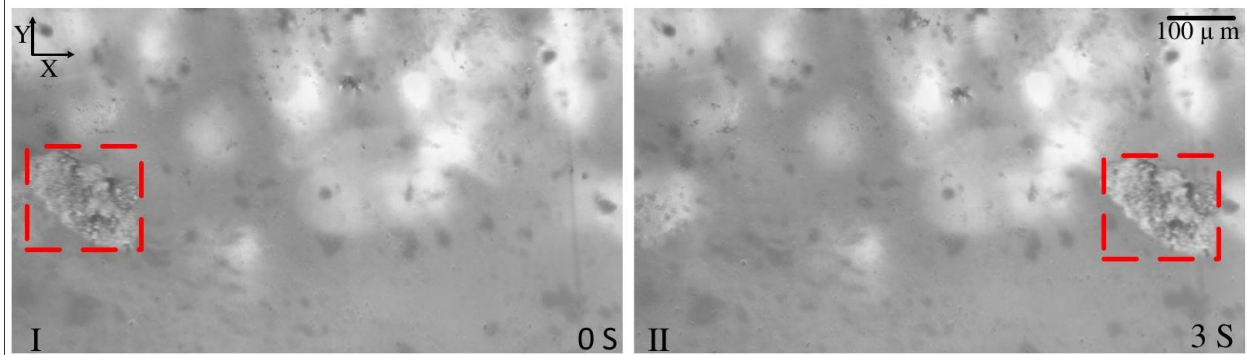


Figure 0.4 Micro-robot of Fe_3O_4 particles motion around the X-axis by using X-axis coils

In the experiment, we energize the X-axis coil for movement. In figure 5.4 shown its demonstration. At $t=0$ sec when no force is applied. Then at $t=3$ sec and it reaches the (+) x-axis. Microrobot covers the 1490 μm in 3 sec its velocity is 496.67 $\mu\text{m/Sec}$.

Conclusion

There are kinds of motion that are possible by using a 2D magnetic micro-robotics system. Rotational motion by using a uniform magnetic field and linear motion for microrobots by using uniform magnetic gradients. Here we show both motion rotation around the 90° and linear motion toward the excitation on axis .

CONCLUSION

In this thesis, we studied the dependence of the magnetic field on the parameters of magnetic actuators. The collinear and planar alignment of magnetic actuators is incredibly important to obtain an optimized magnetic field. Prototype 2D magnetic systems were built and tested. The results showed that the magnitude of the misaligned magnetic actuators is not optimal in the workspace. The plane which is on the central axis of all actuators shows high magnetic field strength and is best for driving magnetic robots.

This work focuses on the use of two-dimensional micro-actuators that can control fully untethered magnetic microrobots. However, two-dimensional can apply controlled magnetic forces and torques in two DOF to tethered equipment, such as magnetically evacuated catheters and tour guides. More importantly, the underlying control strategy presents the ability to estimate exercisable magnetic fields and magnetic field gradients within the system workspace when any electromagnetic field sources are used. Since the use of fewer electromagnets than the number used in the coupled coils is likely to reduce the performance of a converted system, the control strategy may anticipate system limitations. A system can potentially be conceived for catheter guidance in the human heart. In this thesis, we investigated the rotational and linear motion of magnetic micro-robots inside a fluid. It was demonstrated that such liner and rotational motion would locally propel the liner and rotational near the microrobots.

REFERENCES

- [1] “United States of America - Current health expenditure per capita.” .
- [2] N. G. Hockstein, J. P. Nolan, B. W. O’Malley, and Y. J. Woo, “Robotic Microlaryngeal Surgery: A Technical Feasibility Study Using the daVinci Surgical Robot and an Airway Mannequin,” *Laryngoscope*, vol. 115, no. 5, May 2005, doi: 10.1097/01.MLG.0000159202.04941.67.
- [3] A. V. Singh, Z. Hosseinidoust, B.-W. Park, O. Yasa, and M. Sitti, “Microemulsion-Based Soft Bacteria-Driven Microswimmers for Active Cargo Delivery,” *ACS Nano*, vol. 11, no. 10, Oct. 2017, doi: 10.1021/acsnano.7b02082.
- [4] T. Fukuda, F. Arai, and M. Nakajima, *Micro-nanorobotic manipulation systems and their applications*, vol. 9783642363. 2013.
- [5] J. Li, B. Esteban-Fernández de Ávila, W. Gao, L. Zhang, and J. Wang, “Micro/nanorobots for biomedicine: Delivery, surgery, sensing, and detoxification,” *Sci. Robot.*, vol. 2, no. 4, Mar. 2017, doi: 10.1126/scirobotics.aam6431.
- [6] B. Wang, K. Kostarelos, B. J. Nelson, and L. Zhang, “Trends in Micro-/Nanorobotics: Materials Development, Actuation, Localization, and System Integration for Biomedical Applications,” *Adv. Mater.*, vol. 33, no. 4, Jan. 2021, doi: 10.1002/adma.202002047.
- [7] J. J. Abbott, Z. Nagy, F. Beyeler, and B. J. Nelson, “Robotics in the Small, Part I: Microbotics,” *IEEE Robot. Autom. Mag.*, vol. 14, no. 2, Jun. 2007, doi: 10.1109/MRA.2007.380641.
- [8] A. Ferreira, C. Cassier, and S. Hirai, “Automatic Microassembly System Assisted by Vision Servoing and Virtual Reality,” *IEEE/ASME Trans. Mechatronics*, vol. 9, no. 2, Jun. 2004, doi: 10.1109/TMECH.2004.828655.
- [9] H. Ishihara and T. Fukuda, “Dynamical reconfiguration method of cellular robotic system based on distance evaluation,” *Rob. Auton. Syst.*, vol. 19, no. 1, Nov. 1996, doi: 10.1016/S0921-8890(96)00037-1.
- [10] L. Feng *et al.*, “High-speed delivery of microbeads in microchannel using magnetically driven microtool,” Jun. 2011, doi: 10.1109/TRANSDUCERS.2011.5969431.
- [11] S. Sanchez, A. A. Solovev, S. M. Harazim, and O. G. Schmidt, “Microbots Swimming in the Flowing Streams of Microfluidic Channels,” *J. Am. Chem. Soc.*, vol. 133, no. 4, Feb. 2011, doi: 10.1021/ja109627w.
- [12] W. Gao and J. Wang, “The Environmental Impact of Micro/Nanomachines: A Review,” *ACS Nano*, vol. 8, no. 4, Apr. 2014, doi: 10.1021/nn500077a.
- [13] X. Yan *et al.*, “Magnetite Nanostructured Porous Hollow Helical Microswimmers for Targeted Delivery,” *Adv. Funct. Mater.*, vol. 25, no. 33, Sep. 2015, doi: 10.1002/adfm.201502248.
- [14] “Nanoparticle.” www.britannica.com/science/nanoparticle.
- [15] Z. Ren, W. Hu, X. Dong, and M. Sitti, “Multi-functional soft-bodied jellyfish-like swimming,” *Nat. Commun.*, vol. 10, no. 1, Dec. 2019, doi: 10.1038/s41467-019-10549-7.

- [16] I. C. Yasa, A. F. Tabak, O. Yasa, H. Ceylan, and M. Sitti, "3D-Printed Microrobotic Transporters with Recapitulated Stem Cell Niche for Programmable and Active Cell Delivery," *Adv. Funct. Mater.*, vol. 29, no. 17, Apr. 2019, doi: 10.1002/adfm.201808992.
- [17] M. Li *et al.*, "Flexible magnetic composites for light-controlled actuation and interfaces," *Proc. Natl. Acad. Sci.*, vol. 115, no. 32, Aug. 2018, doi: 10.1073/pnas.1805832115.
- [18] H. Ceylan, I. C. Yasa, U. Kilic, W. Hu, and M. Sitti, "Translational prospects of untethered medical microrobots," *Prog. Biomed. Eng.*, vol. 1, no. 1, Jul. 2019, doi: 10.1088/2516-1091/ab22d5.
- [19] M. Kharboutly, M. Gauthier, and N. Chaillet, "Modeling the trajectory of a microparticle in a dielectrophoresis device," *J. Appl. Phys.*, vol. 106, no. 11, Dec. 2009, doi: 10.1063/1.3257167.
- [20] A. A. Solovev, Y. Mei, E. Bermúdez Ureña, G. Huang, and O. G. Schmidt, "Catalytic Microtubular Jet Engines Self-Propelled by Accumulated Gas Bubbles," *Small*, vol. 5, no. 14, Jul. 2009, doi: 10.1002/smll.200900021.
- [21] L.-A. Liew, V. M. Bright, M. L. Dunn, J. W. Daily, and R. Raj, "Development of SiCN ceramic thermal actuators," doi: 10.1109/MEMSYS.2002.984340.
- [22] S. Martel *et al.*, "MRI-based Medical Nanorobotic Platform for the Control of Magnetic Nanoparticles and Flagellated Bacteria for Target Interventions in Human Capillaries," *Int. J. Rob. Res.*, vol. 28, no. 9, Sep. 2009, doi: 10.1177/0278364908104855.
- [23] W. Gao, A. Pei, and J. Wang, "Water-Driven Micromotors," *ACS Nano*, vol. 6, no. 9, Sep. 2012, doi: 10.1021/nn303309z.
- [24] L. Zhang, J. J. Abbott, L. Dong, B. E. Kratochvil, D. Bell, and B. J. Nelson, "Artificial bacterial flagella: Fabrication and magnetic control," *Appl. Phys. Lett.*, vol. 94, no. 6, Feb. 2009, doi: 10.1063/1.3079655.
- [25] I. S. M. Khalil, M. P. Pichel, L. Abelman, and S. Misra, "Closed-loop control of magnetotactic bacteria," *Int. J. Rob. Res.*, vol. 32, no. 6, May 2013, doi: 10.1177/0278364913479412.
- [26] T. Xu, G. Hwang, N. Andreff, and S. Regnier, "Planar Path Following of 3-D Steering Scaled-Up Helical Microswimmers," *IEEE Trans. Robot.*, vol. 31, no. 1, Feb. 2015, doi: 10.1109/TRO.2014.2380591.
- [27] H. Ceylan, J. Giltinan, K. Kozielski, and M. Sitti, "Mobile microrobots for bioengineering applications," *Lab Chip*, vol. 17, no. 10, pp. 1705–1724, 2017, doi: 10.1039/c7lc00064b.
- [28] C. Bouyer *et al.*, "A Bio-Acoustic Levitational (BAL) Assembly Method for Engineering of Multilayered, 3D Brain-Like Constructs, Using Human Embryonic Stem Cell Derived Neuro-Progenitors," *Adv. Mater.*, vol. 28, no. 1, Jan. 2016, doi: 10.1002/adma.201503916.
- [29] S. Li *et al.*, "Application of an acoustofluidic perfusion bioreactor for cartilage tissue engineering," *Lab Chip*, vol. 14, no. 23, 2014, doi: 10.1039/C4LC00956H.
- [30] J. Feng, J. Yuan, and S. K. Cho, "Micropropulsion by an acoustic bubble for navigating microfluidic spaces," *Lab Chip*, vol. 15, no. 6, 2015, doi: 10.1039/C4LC01266F.
- [31] N. Takahashi, Z. Wang, M. A. Rahman, J. Cheng, and A. T. Ohta, "Automated micro-object caging using bubble microrobots," *2016 IEEE 11th Annu. Int. Conf. Nano/Micro Eng. Mol. Syst. NEMS 2016*, pp. 237–240, 2016, doi: 10.1109/NEMS.2016.7758241.

- [32] M. A. Rahman, J. Cheng, and A. T. Ohta, "Parallel actuation and independent addressing of many bubble microrobots," *2016 IEEE 11th Annu. Int. Conf. Nano/Micro Eng. Mol. Syst. NEMS 2016*, pp. 279–282, 2016, doi: 10.1109/NEMS.2016.7758250.
- [33] P. Fischer and A. Ghosh, "Magnetically actuated propulsion at low Reynolds numbers: towards nanoscale control," *Nanoscale*, vol. 3, no. 2, 2011, doi: 10.1039/C0NR00566E.
- [34] J. Hwang, J. Kim, and H. Choi, "A review of magnetic actuation systems and magnetically actuated guidewire- and catheter-based microrobots for vascular interventions," *Intell. Serv. Robot.*, vol. 13, no. 1, Jan. 2020, doi: 10.1007/s11370-020-00311-0.
- [35] W. Stone, "Alloplasty in Surgery of the Eye," *N. Engl. J. Med.*, vol. 258, no. 12, Mar. 1958, doi: 10.1056/NEJM195803202581206.
- [36] D. Kostoff, "Protoplasmic viscosity in plants," *Protoplasma*, vol. 11, no. 1, Dec. 1930, doi: 10.1007/BF01614329.
- [37] Z. Yang and L. Zhang, "Magnetic Actuation Systems for Miniature Robots: A Review," *Adv. Intell. Syst.*, vol. 2, no. 9, p. 2000082, 2020, doi: 10.1002/aisy.202000082.
- [38] S. Kolachalama and S. Lakshmanan, "Continuum Robots for Manipulation Applications: A Survey," *J. Robot.*, vol. 2020, Jul. 2020, doi: 10.1155/2020/4187048.
- [39] G. Caprari, "Autonomous Micro-Robots : Applications and Limitations," no. March, 2014, doi: 10.5075/epfl-thesis-2753.
- [40] H. Choi, J. Choi, G. Jang, J. O. Park, and S. Park, "T[1] H. Choi, J. Choi, G. Jang, J. O. Park, and S. Park, 'Two-dimensional actuation of a microrobot with a stationary two-pair coilsystem,' *Smart Mater. Struct.*, vol. 18, no. 5, 2009, doi: 10.1088/0964-1726/18/5/055007.wo-dimensional actuation of a micror," *Smart Mater. Struct.*, vol. 18, no. 5, 2009, doi: 10.1088/0964-1726/18/5/055007.
- [41] C. Chen, F. Soto, E. Karshalev, J. Li, and J. Wang, "Hybrid Nanovehicles: One Machine, Two Engines," *Adv. Funct. Mater.*, vol. 29, no. 2, Jan. 2019, doi: 10.1002/adfm.201806290.
- [42] W. Gao, K. M. Manesh, J. Hua, S. Sattayasamitsathit, and J. Wang, "Hybrid Nanomotor: A Catalytically/Magnetically Powered Adaptive Nanowire Swimmer," *Small*, vol. 7, no. 14, Jul. 2011, doi: 10.1002/smll.201100213.
- [43] L. Ren, D. Zhou, Z. Mao, P. Xu, T. J. Huang, and T. E. Mallouk, "Rheotaxis of Bimetallic Micromotors Driven by Chemical–Acoustic Hybrid Power," *ACS Nano*, vol. 11, no. 10, Oct. 2017, doi: 10.1021/acsnano.7b06107.
- [44] C. Chen *et al.*, "Chemical/Light-Powered Hybrid Micromotors with 'On-the-Fly' Optical Brakes," *Angew. Chemie Int. Ed.*, vol. 57, no. 27, Jul. 2018, doi: 10.1002/anie.201803457.
- [45] J. Li *et al.*, "Magneto–Acoustic Hybrid Nanomotor," *Nano Lett.*, vol. 15, no. 7, Jul. 2015, doi: 10.1021/acs.nanolett.5b01945.
- [46] C. Heunis, J. Sikorski, and S. Misra, "Flexible Instruments for Endovascular Interventions: Improved Magnetic Steering, Actuation, and Image-Guided Surgical Instruments," *IEEE Robot. Autom. Mag.*, vol. 25, no. 3, Sep. 2018, doi: 10.1109/MRA.2017.2787784.

- [47] G. Ciuti, P. Valdastri, A. Menciassi, and P. Dario, "Robotic magnetic steering and locomotion of capsule endoscope for diagnostic and surgical endoluminal procedures," *Robotica*, vol. 28, no. 2, Mar. 2010, doi: 10.1017/S0263574709990361.
- [48] P. Valdastri *et al.*, "Magnetic air capsule robotic system: proof of concept of a novel approach for painless colonoscopy," *Surg. Endosc.*, vol. 26, no. 5, May 2012, doi: 10.1007/s00464-011-2054-x.
- [49] A. W. Mahoney and J. J. Abbott, "Five-degree-of-freedom manipulation of an untethered magnetic device in fluid using a single permanent magnet with application in stomach capsule endoscopy," *Int. J. Rob. Res.*, vol. 35, no. 1–3, Jan. 2016, doi: 10.1177/0278364914558006.
- [50] Z. Yang and L. Zhang, "Magnetic Actuation Systems for Miniature Robots: A Review," *Adv. Intell. Syst.*, vol. 2, no. 9, Sep. 2020, doi: 10.1002/aisy.202000082.
- [51] F. Carpi and C. Pappone, "Stereotaxis Niobe[®] magnetic navigation system for endocardial catheter ablation and gastrointestinal capsule endoscopy," *Expert Rev. Med. Devices*, vol. 6, no. 5, Sep. 2009, doi: 10.1586/erd.09.32.
- [52] M. E. Alshafeei, A. Hosney, A. Klingner, S. Misra, and I. S. M. Khalil, "Magnetic-based motion control of a helical robot using two synchronized rotating dipole fields," *Proc. IEEE RAS EMBS Int. Conf. Biomed. Robot. Biomechanics*, pp. 151–156, 2014, doi: 10.1109/biorob.2014.6913768.
- [53] Wei Zhang, Yonggang Meng, and Ping Huang, "A Novel Method of Arraying Permanent Magnets Circumferentially to Generate a Rotation Magnetic Field," *IEEE Trans. Magn.*, vol. 44, no. 10, Oct. 2008, doi: 10.1109/TMAG.2008.2002505.
- [54] C. Huang, T. Xu, J. Liu, L. Manamanchaiyaporn, and X. Wu, "Visual Servoing of Miniature Magnetic Film Swimming Robots for 3-D Arbitrary Path Following," *IEEE Robot. Autom. Lett.*, vol. 4, no. 4, Oct. 2019, doi: 10.1109/LRA.2019.2931234.
- [55] J. J. Abbott, Z. Nagy, F. Beyeler, and B. J. Nelson, "Robotics in the Small, Part I: Microbotics," *IEEE Robot. Autom. Mag.*, vol. 14, no. 2, pp. 92–103, 2007, doi: 10.1109/mra.2007.380641.
- [56] S. Jeong, H. Choi, J. Choi, C. Yu, J. Park, and S. Park, "Novel electromagnetic actuation (EMA) method for 3-dimensional locomotion of intravascular microrobot," *Sensors Actuators A Phys.*, vol. 157, no. 1, Jan. 2010, doi: 10.1016/j.sna.2009.11.011.
- [57] C. Yu *et al.*, "Novel electromagnetic actuation system for three-dimensional locomotion and drilling of intravascular microrobot," *Sensors Actuators, A Phys.*, vol. 161, no. 1–2, pp. 297–304, 2010, doi: 10.1016/j.sna.2010.04.037.
- [58] I. S. M. Khalil, H. C. Dijkslag, L. Abelmann, and S. Misra, "MagnetoSperm: A microrobot that navigates using weak magnetic fields," *Appl. Phys. Lett.*, vol. 104, no. 22, Jun. 2014, doi: 10.1063/1.4880035.
- [59] S. Salmanipour and E. Diller, "Eight-degrees-of-freedom remote actuation of small magnetic mechanisms," *Proc. - IEEE Int. Conf. Robot. Autom.*, pp. 3608–3613, 2018, doi: 10.1109/ICRA.2018.8461026.
- [60] D. Son, X. Dong, and M. Sitti, "A Simultaneous Calibration Method for Magnetic Robot Localization and Actuation Systems," *IEEE Trans. Robot.*, vol. 35, no. 2, pp. 343–352, 2019, doi: 10.1109/TRO.2018.2885218.

- [61] E. Diller and M. Sitti, “Three-Dimensional Programmable Assembly by Untethered Magnetic Robotic Micro-Grippers,” *Adv. Funct. Mater.*, vol. 24, no. 28, Jul. 2014, doi: 10.1002/adfm.201400275.
- [62] I. S. M. Khalil, V. Magdanz, S. Sanchez, O. G. Schmidt, and S. Misra, “Three-dimensional closed-loop control of self-propelled microjets,” *Appl. Phys. Lett.*, vol. 103, no. 17, Oct. 2013, doi: 10.1063/1.4826141.
- [63] J. Li *et al.*, “Magnetic Micromachine Using Nickel Nanoparticles for Propelling and Releasing in Indirect Assembly of Cell-Laden Micromodules,” *Micromachines*, vol. 10, no. 6, Jun. 2019, doi: 10.3390/mi10060370.
- [64] E. Diller, J. Giltinan, G. Z. Lum, Z. Ye, and M. Sitti, “Six-degree-of-freedom magnetic actuation for wireless microrobotics,” *Int. J. Rob. Res.*, vol. 35, no. 1–3, Jan. 2016, doi: 10.1177/0278364915583539.
- [65] M. P. Kummer, J. J. Abbott, B. E. Kratochvil, R. Borer, A. Sengul, and B. J. Nelson, “Octomag: An electromagnetic system for 5-DOF wireless micromanipulation,” *IEEE Trans. Robot.*, vol. 26, no. 6, pp. 1006–1017, 2010, doi: 10.1109/TRO.2010.2073030.
- [66] T. Greigarn, R. Jackson, T. Liu, and M. C. Cavusoglu, “Experimental validation of the pseudo-rigid-body model of the MRI-actuated catheter,” May 2017, doi: 10.1109/ICRA.2017.7989414.
- [67] C. Pawashe, S. Floyd, and M. Sitti, “Multiple magnetic microrobot control using electrostatic anchoring,” *Appl. Phys. Lett.*, vol. 94, no. 16, Apr. 2009, doi: 10.1063/1.3123231.
- [68] H. Kim, J. Ali, U. K. Cheang, J. Jeong, J. S. Kim, and M. J. Kim, “Micro Manipulation Using Magnetic Microrobots,” *J. Bionic Eng.*, vol. 13, no. 4, pp. 515–524, 2016, doi: 10.1016/S1672-6529(16)60324-4.
- [69] E. Diller, S. Miyashita, and M. Sitti, “Remotely addressable magnetic composite micropumps,” *RSC Adv.*, vol. 2, no. 9, 2012, doi: 10.1039/c2ra01318e.
- [70] A. Kotikian *et al.*, “Untethered soft robotic matter with passive control of shape morphing and propulsion,” *Sci. Robot.*, vol. 4, no. 33, Aug. 2019, doi: 10.1126/scirobotics.aax7044.
- [71] M. Field, “Coils for Magnetic Field Creation,” pp. 174–188.
- [72] “[https://en.wikipedia.org/wiki/Permeability_\(electromagnetism\)](https://en.wikipedia.org/wiki/Permeability_(electromagnetism)).”
- [73] K. Simeonidis *et al.*, “Development of iron-based nanoparticles for Cr(VI) removal from drinking water,” *EPJ Web Conf.*, vol. 40, Jan. 2013, doi: 10.1051/epjconf/20134008007.